ELECTRO CHEMICAL SPARK MACHINING USING ABRASIVE CUTTING TOOLS

A Thesis Submitted

in Partial Fulfillment of the Requirement

for the Degree of

MASTER OF TECHNOLOGY

by

K. MASA RAMESH

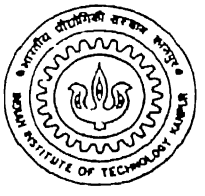

to the

DEPARTMENT OF MECHANICAL ENGINEERING

INDIAN INSTITUTE OF TECHNOLOGY - KANPUR

NOV 1998.

CERTIFICATE

It is certified that the work contained in the thesis entitled **ELECTROCHEMICAL SPARK MACHINING USING ABRASIVE CUTTING TOOLS** , by Mr. **K. MASA RAMESH,** has been carried out under our supervision and that this work has not been submitted elsewhere for a degree.

(Prof. S. K. Chaudhury)

Deptt. of Mech. Engg.

Indian Institute of Technology

Kanpur 208 016, India

(Prof. V. K. Jain)

Deptt. of Mech. Engg.

Indian Institute of Technology

Kanpur 208 016, India

27 NOV 1998

Acknowledgments

I take this opportunity to express the heart felt gratitude towards my thesis supervisors Prof. V K Jain and Prof. S. K. chaudhury for their expert guidance, encouragement, and suggestions which have been critical factors in successful completion of the present work. I am very thankful to Department of Science and Technology for financial assistance towards this project. I would like to thank WIDIA (INDIA) LTD for providing alumina specimens for my experimental work.

I am very grateful to the staff of manufacturing science laboratory, Mr. R.M.Jha, Mr. Namdev, and Mr. Sharma for their help during experimental work. I am very thankful to Mr. P.K.paul, for his help in taking SEM photographs.

I am very thankful to Shivaram, Rajani, Prabhudas, Kosiva, Sai, Iv, Santosh, R K Jain, Classy and all my other friends for their encouragement, suggestions and help during the experimentation. I also take this opportunity to thank my class mates, juniors and other friends.

I am greatly indebted to my parents, who encouraged me throughout to go for higher studies in spite of having many problems.

K. MASA RAMESH

Abstract

Electrically non - conducting hard and brittle materials like alumina and glass are becoming popular because of their inert nature, high hardness and refractoriness. Machining of these kind of materials by conventional processes are not possible. And non traditional machining methods such as, ECM and EDM can't be used for the machining of this class of materials. Therefore there is a need to develop a process which is capable of machining these materials. Lately electrochemical spark machining (ECSM) process is being developed to machine this class of materials.

The work attempted in this thesis is the machining of electrically non-conducting hard, brittle and high temperature resistant materials by employing ECSM process using eccentrically rotating abrasive cutting tool. So far, only solid ordinary cutting tools have been used by previous researchers and the results obtained by them are not very encouraging.

In the present work orbital rotational of the abrasive cutting tool has shown the encouraging results. Process performance has been improved for both the materials (alumina and borosillicate glass), with the abrasive tool when compared to ordinary cutting tool. During experimentation it was observed that, beyond a certain value of electrolyte temperature the process performance deteriorated.

Contents

List of Figures

List of Tables

Nomenclature

w/p	work piece
ACT	Abrasive cutting tool
OCT	Ordinary cutting tool
BSG	Borosillicate glass
SEM	Scanning electron microscopic

Chapter -1

Introduction

1. 1 Introduction

Electrically non-conducting materials are becoming increasingly popular because of their inert nature, high hardness and refractoriness. Non traditional machining methods like ECM and EDM can't be used for machining of this class of materials. Glass and ceramics come under this class of materials. Production of glass and ceramics need not only the processes such as casting, compacting, melting, forming and sintering but also the machining processes such as grinding and polishing to impart the required final accuracy. For the production of small number of parts, it is not economical to use mass production techniques such as casting and sintering. Therefore, the field of utilisation of these materials has remained comparatively narrow.

Diamond grinding, ultrasonic machining (USM), abrasive jet machining (AJM), abrasive water jet machininig (AWJM), laser beam machining (LBM), and ion beam machining (IBM) are those processes which can be used for machining these hard, brittle and electrically non-conducting materials. But these processes have some limitations.

Lately electro chemical spark machining (ECSM) process is being employed for machining of electrically non-conducting materials like ceramics and glass. ECSM is a process in which material removal is accomplished by establishing sparks in the vicinity of the work piece in electrolyte. Major limitation of the ECSM process is very low penetration depth. This has been partially overcome by the use of an orbital rotational tool [1] in ECSM process. In this research work, an hybrid process has been proposed to explore the possibility of further improving the material removal during ECSM. The work reported in this thesis on electro chemical spark abrasive drilling (ECSAD) is, based on the ECSM process. ECSAD uses abrasives impregnated tool during machining operation.

An electrochemical spark machining set-up consists of two electrodes dipped in electrolyte, one of which is the tool of the desired shape and the other one as a flat plate made of graphite. When an external potential is applied between the electrodes, the electric current flows through the electrolyte resulting in electrochemical reactions such as anodic dissolution, cathodic deposition, electrolysis of electrolyte etc., depending upon the electrode-electrolyte combination. Electrolytic cell can exhibit any of the following three different phenomena namely, electrochemical action only (as in normal ECM), electro chemical action followed by discharge between electrodes, electrochemical action followed by discharge between electrode and electrolyte. It has been observed that the sparking occurs at the smaller electrode above a certain voltage for a particular electrolyte. This sparking is not between the electrodes, but across a hydrozen gas bubble [2]. This is known as the Electro Chemical Discharge (ECD) phenomenon. If the workpiece is brought in the vicinity of spark zone, machining would takes place. Fig 1.1 shows the ECSM set-up.

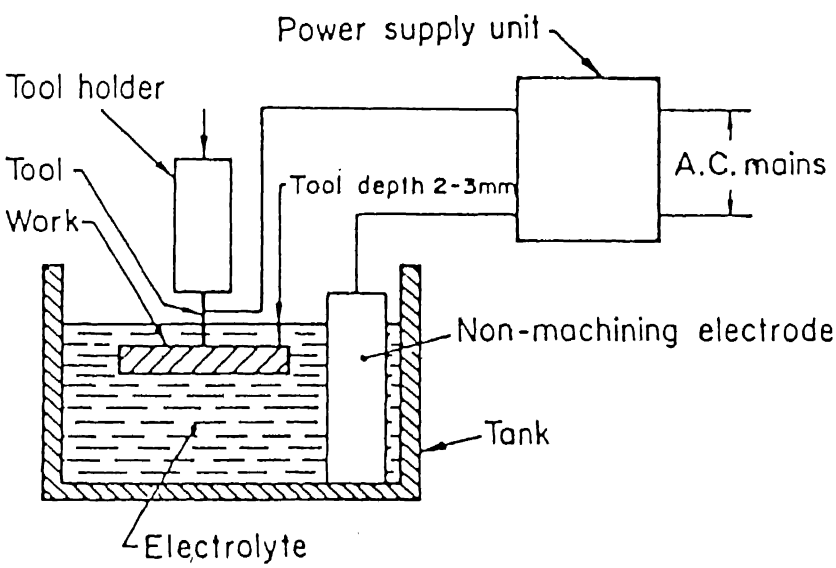

Fig 1.1 : Configuration of non conducting work piece machining using ECSM [3]

1.2 Literature Review

Electrochemical spark during electrolysis of molten Nacl at high current density, was first observed by Taylor in 1925 at the anode tip and was termed as "Anode effect". Later Kellog in 1950 showed that similar phenomenon can occuur at the cathode and also during electrolysis of an aqueous electrolyte. Kurafugi and suda in 1968 drilled holes in glass using such electric discharge.

In 1984, T.Suchiya *et al* [4] used wire electrochemical discharge for machining glass and ceramics. The method is a combination of wire-EDM and ECSM. They used 25Hz rectangular pulse with 80% duty factor, NaoH and KoH as electrolyte, galss specimen of 1.2mm thickness as work piece, wire of dia 0.2mm as electrode and it is driven with a speed of 60 cm/min in experiments. They have concluded that glass and ceramic plates can be slotted successfully.

Crichton and Mcgeough [5] studied in 1985, the mechanism of discharge in electro chemical arc machining. They reported that electrochemical spark occurs between cathode electrode and electrolyte solution through bubbles formed by electrochemical reaction. On the other hand, an arc discharge is formed when spark grows to bridge the gap between the electrodes. Spark discharge has no effect on the material removal while arc discharge leaves a crater on surface.

Rao *et al.* [6] investigated Travelling wire Electrochemical Spark Machining (TW-ECSM) of composites. They reported similar effects of voltage on MRR, TWR and overcut as reported by Tandon *etal* [ ]. Increase in NaoH concentration, increases MRR, TWR and overcut up to 20% concentration. Beyond this concentration, the values of thease responses decrease, primarily because the value of specific conductance beyond approximately 20% concentration decreases. Effect of bubbles on ECSM process was also studied by introducing artificially produced bubbles. It resulted in lower MRR because most of the bubbles died out without sparking. However, accuracy of the machined component was found to be better.

Allesu *et al* [7], have made some investigations into spark machining of non conducting materials. They carried out the experiments mainly on glass samples by varying voltage, electrolyte temperature and electrolyte concentration.They also studied the effect of tool size, shape and material on material removal rate. They concluded that with increase in applied voltage m.r.r increases. However beyond a certain value of applied voltage cracks were observed on glass surface. They explained it as due to higher thermal input and subsequent thermal cracking of glass. They used NaCl, NaOH and KOH solutions as electrolytes for evaluating their performance in machining. Among these electrolytes NaOH solution was found to perform better. Regarding the effect of electrolyte concentration on m.r.r., it increases with increase in concentration. Similarly material removal rate showed a linear relationship with temperature of electrolyte. Machining has been performed for a period of 1min. Higher temperature yielded higher m.r.r. They have also tried tools with different diameters and shapes (solid and hollow) and made of different materials. It was found that lesser the cross sectional area of the tool, better was the performance. Hollow tools gave better performance than solid tools, stainless steel showed very good results as tool material.

Naveen Gautam *et al* [1] did experiments with different tool kinematics like stationary tool, rotating tool with or without electrolyte flow through it, tool with orbital rotation and upward movement of work piece. They showed that rotation of tool and flow of electrolyte through the tool have improved the process performance up to some level. They have concentrated on borosilicate glass and did some experiments on quartz. Through holes were drilled successfully in quartz glass plates using total discharge configuration.

Indrajit Basak [2] conducted experiments on ECD and ECDM. He developed a quantitative model predicting the critical voltage and critical current to initiate the spark. He has also developed a model to predict MRR in ECDM for certain given conditions. It was pointed out that the critical current is a function of equivalent surface area of the tool electrode. He has concluded that electrical discharge takes place due to switching action and not due to dielectric breakdown of the medium, i.e, electrolyte. It has also been suggested that for rough machining operations, an inductance should be introduced in the circuit because of which two hundred percent increase in MRR can be achieved.

Y.P Singh *et al* have [8] designed and fabricated a travelling wire electrochemical spark machine and conducted experiments with partially electrically conducting materials like piezoelectric ceramics (PZT) and carbon fiber reinforced epoxy composites. They studied the effect of variation in voltage and electrolyte concentration on MRR and overcut.

Nesarikar *et al.* [9] carried out TW-ECSM for slicing of kelvar -epoxy composites. Electrolyte conductivity, voltage and specimen thickness were taken as independent parameters while material removal rate, diametral over cut and work piece damage were taken as responses. During their work, electrolyte flushing was also tried successfully. The objective was to limit the variation in electrolyte temperature and to remove the debris of work piece and graphite from the electrolyte tank.

Raghuram *et al.* [10] studied the effect of various circuit parameters on electrolytes in the electrochemical discharge phenomenon. They showed that external circuit parameters have a definite influence on the discharge characteristics. Internal inductance and capacitance in the electrolytes are observed with the application of rectified and smooth DC voltages. The introduction of an external inductor on the circuit has the advantage of supplying a constant power input to the cell .

Recently Sanjay chak [11] has conducted experiments on machining of alumina and quartz by ECSM process. He also studied the effect of supply voltage and electrolyte temperature on MR. He has shown that MR is found to increase with increasing supply voltage and electrolyte temperature.

1.3 Objectives of the Present Work

In earlier research work on ECSM process, only ordinary cutting tools have been used. In order to enhance the capabilities of the process, in the present work abrasive cutting tools have used and the performance has been compared, with the ECSM process with non abrasive tools. The following are the main objectives of this work.

- To explore the possibility of enhancing the material removal by using abrasive cutting tools.
- Comparing the results obtained by both processes.
- To find out the feasibility of using ECSAD process for two different materials namely borosilicate glass and alumina.
- Scanning electron microscopic analysis of the machined surface and the used cutting tools.

Chapter - 2

Experimental set-up and Procedure

2.1 Experimental Set-up

Experimental set-up shown in Fig 2.1 is used for Electro chemical Spark drilling (ECSD) of non-conducting materials, designed and fabricated by Gautam Jain [1]. In this set-up, two independent stepper motors are used with suitable independent "unistep" controllers for the drive system. One is used for giving feed to the workpiece and another is used for tool rotation. Work feed stepper motor is 12V, 20 kg-cm torque and tool rotation stepper motor is of 12V and 7 kg-cm torque. Feed motor is connected to a worm and worm gear with the transmission ratio of 1:80 and with the help of a screw and nut mechanism the feed is given to the workpiece. The minimum feed which can be provided with reduction gear arrangement is $2\ \mu m/\min$, while the highest feed is 1.2mm/min. Tool rotation motor is directly coupled with hollow pipe whose another end is fixed with adjustable eccentric slide. Beneath this slide a tool holder is attached in which tool is fixed. An aluminium disc is fitted above the adjustable eccentric slide.

Smooth D.C power supply was used, in which the output voltage can be regulated as per the requirements. Continuous power supply was provided to the tool during the rotation, by carbon brush-slip ring arrangement. Spring loaded carbon brush is kept in a perspex casing, which is screw tightened to the lower face of the platform. Experiments have been performed at different voltage levels and at different electrolyte temperatures using sodium hydroxide as electrolyte.

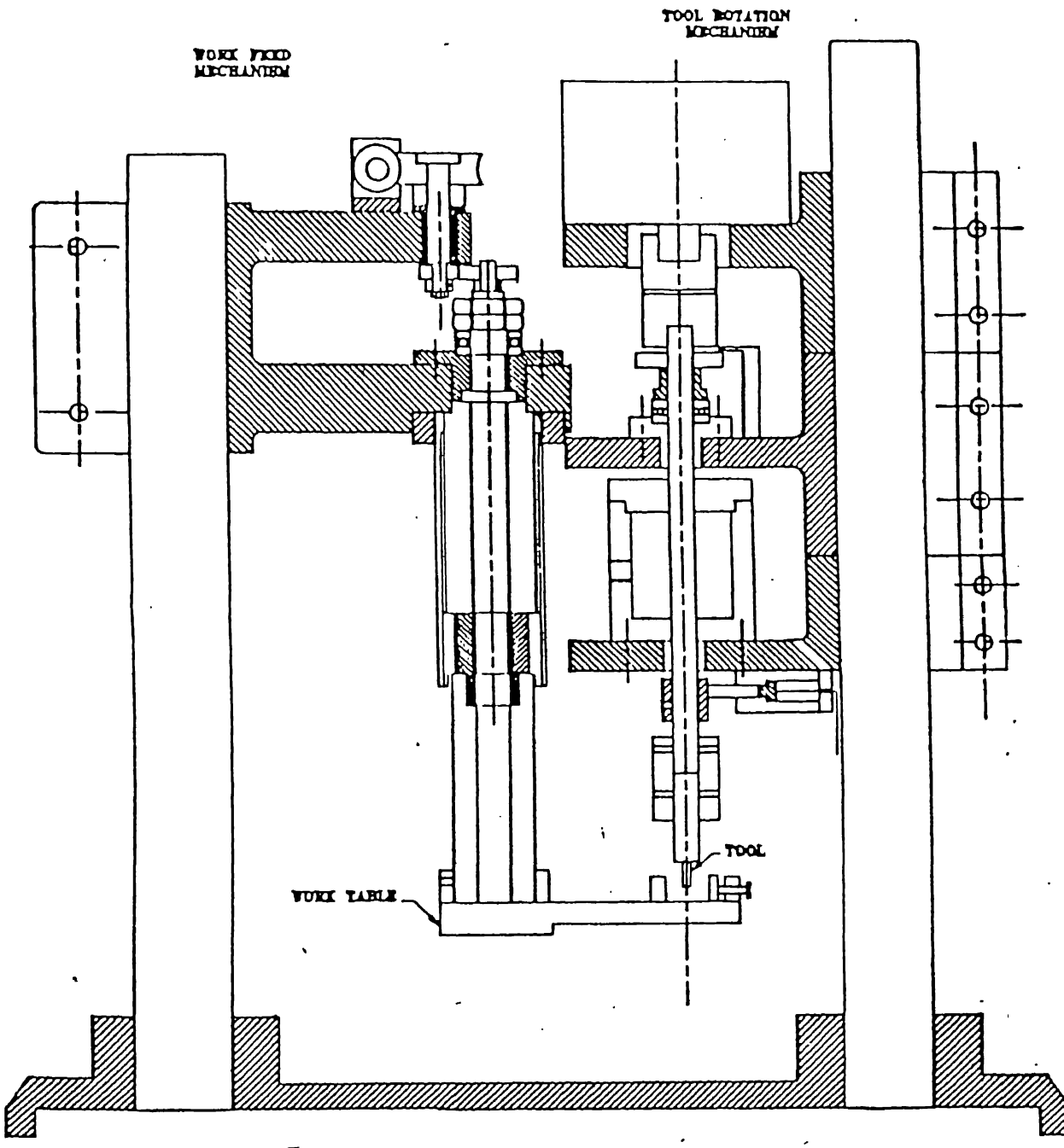

Fig 2.1 : electrochemical spark machine [3]

2.2 Electrolyte

Through out the experiments 22 wt% Sodium Hydroxide(NaoH) solution is used as electrolyte because its conductivity is found to be maximum at this concentration. As most of the previous work has been done using NaoH, so using the same solution as electrolyte would help in comparing the results. Conductivity of electrolyte is measured by digital conductivity meter. This conductivity meter is calibrated initially using a standard solution of known strength of potassium chloride.

2.3 Work Material

The following two electrically non-conducting materials have been used as work materials.

2.3.1 Borosilicate Glass

This glass is used in laboratories as well as for industrial applications where maximum thermal resistance, thermal shock resistance, mechanical resistance as well as unusual chemical resistance are required. Borosilicate glasses constitute á large portion of industrial glasses (laboratory glasses, neutral glasses for pharmacy, glasses for electronics, micro porous glasses etc). Physical and chemical properties of borosillicate glass are given in appendix - A. The diameter of the specimen used was 18.6 mm.

2.3.2 Alumina

Sintered alumina is much less expensive to make as compare to crystalline alumina. It has been widely used at high temperature and in diverse applications such as refractories, lamp tubes, grinding pebbles, polishing compounds, electronic substances, spark plugs, laboratory ware etc. Physical and chemical properties of Alumina are given in appendix - B. The diameter of the specimen used was 9.5 mm. And thease specimens were supplied by WIDIA (INDIA) LTD BANGALORE.

2.4 EXPERIMENTATION

The basic constituents of an ECSM cell were two electrodes of different polarities and the electrolyte. For experimental work the tool is used as negative electrode and the graphite

rod as positive electrode. In the present work two abrasive cutting tools (Fig 2.2) and two ordinary cutting tools were used on two different work piece materials. Ordinary cutting tools were made of mildsteel. The size and shape of the ordinary cutting tools were same as the abrasive cutting tools. The tool rotation was set at 20 rpm since it gives the maximum MRR at that rpm [1]. For the material removal rate to be maximum the eccentricity should be slightly more than the half of the diameter [1]. Therefore, the values were choosen according to the maximum material removal conditions. Tool eccentricity was kept constant through out the experiment. For the present experiments two variables were considered as supply voltage and electrolyte temperature. Through out each of the experiments the temperature of electrolyte was kept constant with the help of an electric heater and thermostat and was counter checked by a thermometer. In case of borosilicate glass each experiment was carried out for 15 min duration. At every 5 min of interval the conductivity of electrolyte was measured in case of glass and at every 15 min in case of alumina. To compensate the boiling of electrolyte, water was added whenever required. At higher temperatures even though water was added, conductivity could not be maintained constant. In case of alumina each experiment was carried out at 30 mins. A minimum level of electrolyte was maintained between the tool tip and work piece because down ward movement of tool gives sparks which result in higher over cut on machined surface. For each experiment fresh electrolyte was prepared so as to improve the accuracy of the experiments. Each and every experiment was conducted with a new cutting tool as well.

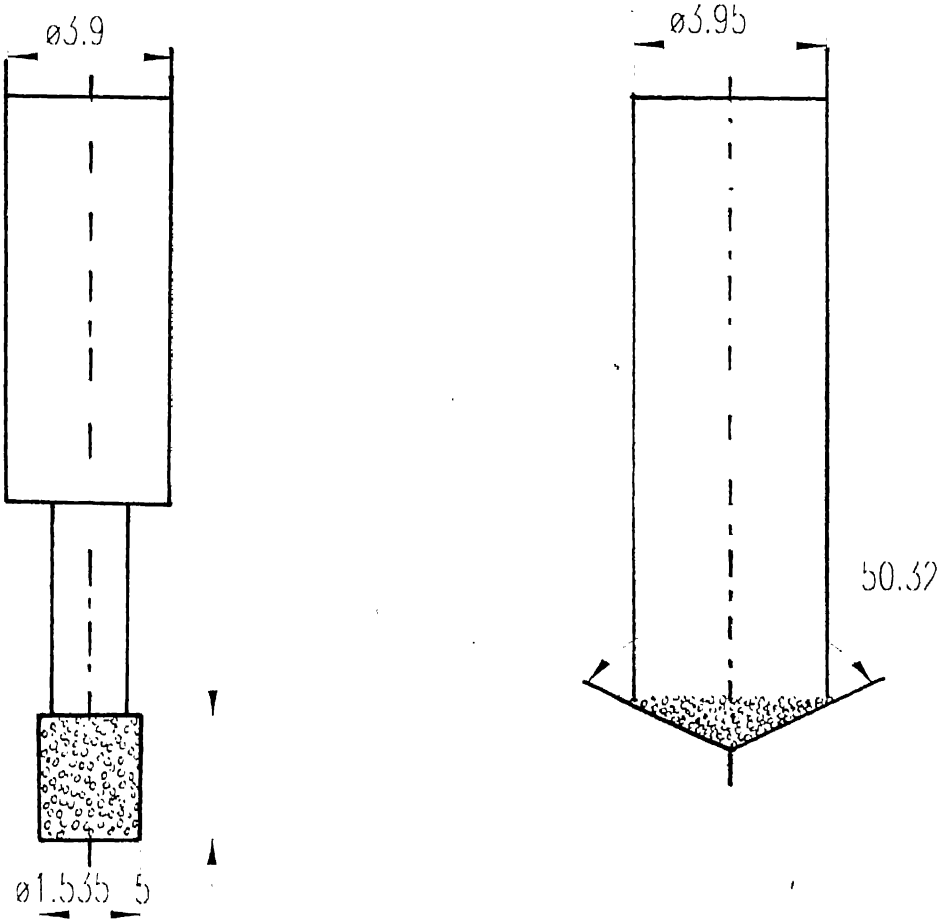

Fig 2.2 : abrasive cutting tools

To find out the amount of feed was a major problem in ECSM process. Earlier work has been done with a constant gap between the tool and work. In this work abrasive cutting tools were used . Therefore for the abrasive action to take place in addition to sparking action, the abrasive cutting tool should be made in contact with the work piece. This was accompolished by a switching arrangement (FIg2.4). In this arrangement an aluminium disc was fitted above the adjustable slide. Tool was gravity fed, and when the tool touches the work piece which is given a feed upwards, the adjustable slide along with disc was lifted up pushing the plunger up ward and the electrical circuit was completed which was indicated by glowing of a bulb. At this

instant feed rate was noted down. To keep the cutting tool always in contact with the w/p, feed rate was given slightly more than the corresponding noted value.

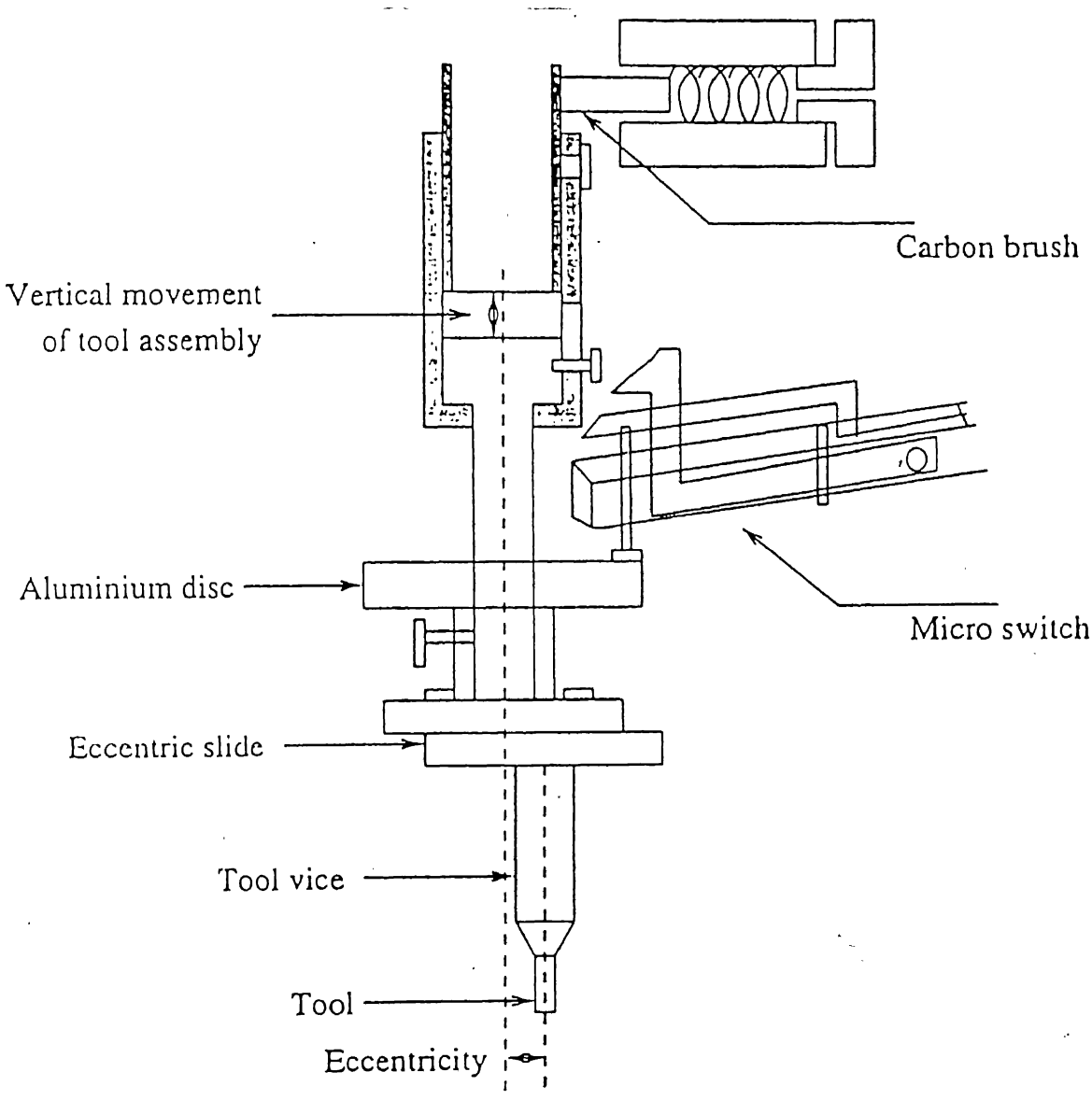

Fig 2.3 : Eccentric Tool Mechanism micro switch arrangement

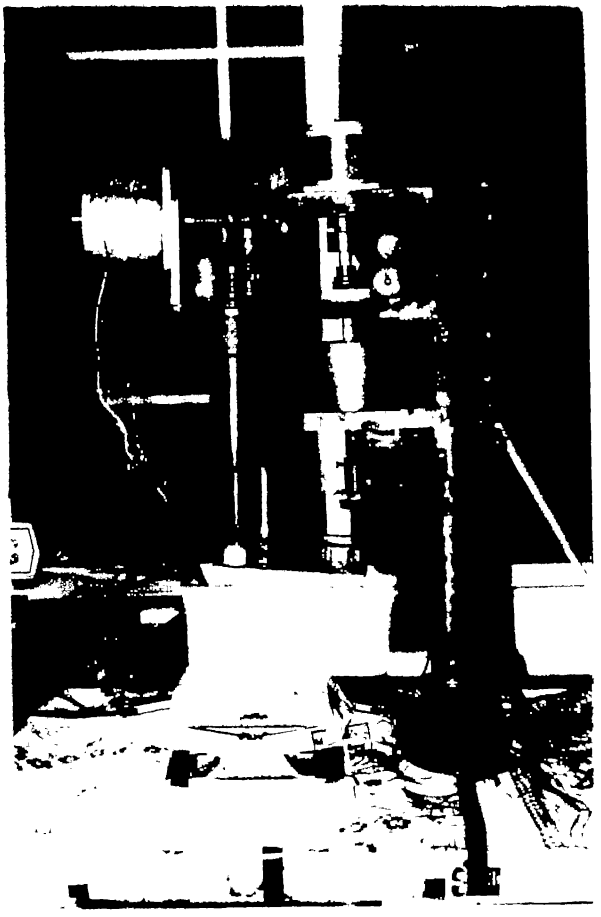

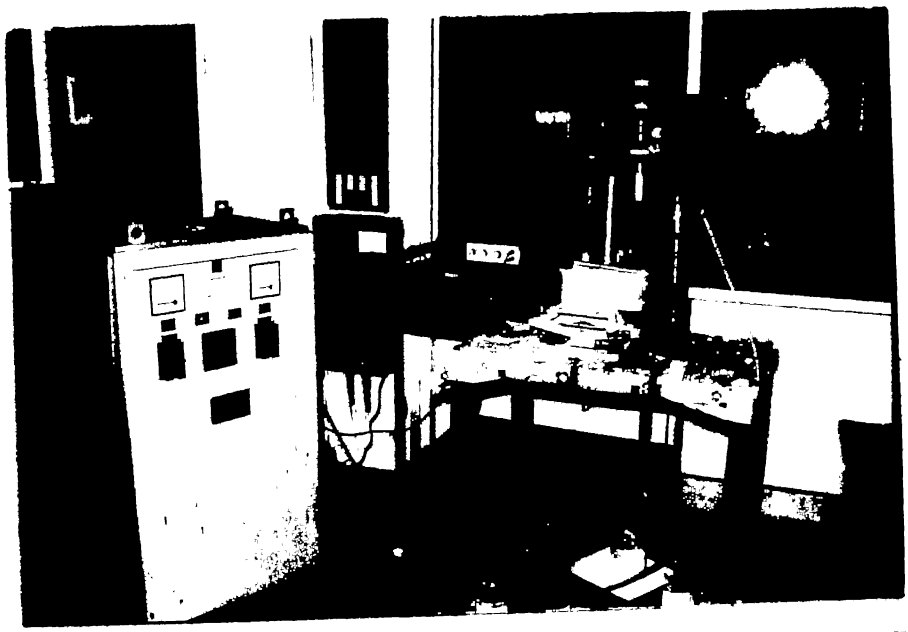

Figure 2.4 : Photographs of experimental set - up

2.5 Material Removal Measurement

The weight of the work piece was measured using the available electronic weight balance "AFCOSET FX-400" having a least count of 0.001g. By measuring the weight of the samples before and after machining, the material removal was calculated after taking their difference.

2.6 Machined Depth Measurement

Machined depth of work piece was measured by a dial guage (Fig 2.5) with a least count of 0.01 mm. Dail gauge was fitted on a stand, work piece was placed on a platform. By suitably moving the work piece the dail indicator stylus was moved in and out of the machined holes. Difference of two readings shows the depth of machining.

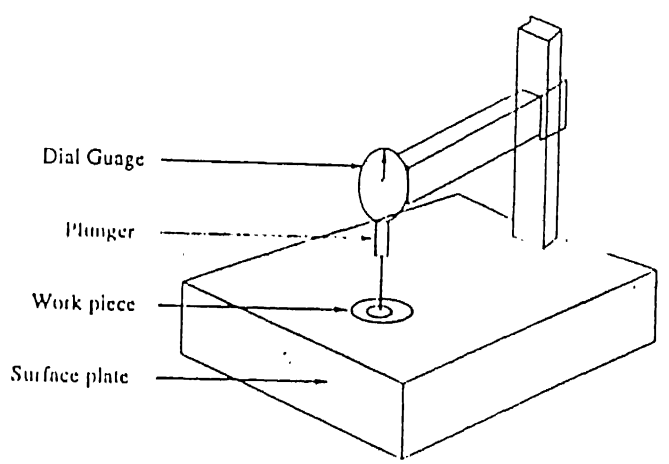

Fig :2.5 Set up for machine depth measurement

2.7 Plan of Experiments

Experiments conducted were planned using statistical techniques so that useful inferences could be obtained by performing minimum number of experiments.The

general form of a quadratic (second degree) polynomial equation is illustrated by the following equation [12].

$$y_u = b_0 + \sum_{i=1}^{k} b_i x_{iu} + \sum_{i=1}^{k} b_i x_{iu}^2 + \sum_{i<j}^{k} b_{ij} x_{iu} x_{ju} \quad \text{.....(2.2)}$$

x_{Iu} represents the level of the I th factor in the u th experiment..

where, k = no. of variables.

x_{iu} ,x_{ju} = Variables.

b_i = Regression constants

y_u = Responce at the u th observation.

The design for two x - variables is shown in Table 2.1.

Table 2.1 Central composite rotatable design for k=2

S.No.	X_0	X_1	X_2	X_1^2	X_2^2	X_1X_2
1	1	-1	-1	1	1	1
2	1	1	-1	1	1	-1
3	1	-1	1	1	1	-1
4	1	1	1	1	1	1
5	1	-1.414	0	2	0	0
6	1	1.414	0	2	0	0
7	1	0	-1.414	0	2	0
8	1	0	1.414	0	2	0
9	1	0	0	0	0	0
10	1	0	0	0	0	0
11	1	0	0	0	0	0
12	1	0	0	0	0	0
13	1	0	0	0	0	0

Subsequent steps are as follows:

1. Complete the columns headed $x_0, x_1, x_2, x_1^2, x_2^2, x_1x_2$ as shown. The two way array with 6 columns and 13 rows comprises the X - matrix of the x-variables. The corresponding values of the response Y are placed on the right.
2. Form the sum of products of each column in the matrix X with the column of Y values. These sum of products are denoted by (0y), (1y), (2y) and so on.
   From the values of (0y), (1y), etc. the regression coefficients* are computed directly from the equations given below [12].

$$b_0 = 0.2(0y) - 0.1\sum iiy$$
$$\sum iiy = (11y) + (22y)$$
$$b_i = 0.125(iy) \qquad \text{.....(2.3.)}$$
$$b_{ii} = 0.125(iiy) + 0.01875\sum(iiy) - 0.1(0y)$$
$$b_{ij} = 0.25(ijy)$$

* In case of alumina regression coefficients were found by using the matrix mathod. The related programme was given in the appendix - C .

In the present analysis of the experiments, the effect of two variables viz. supply voltage (V) and electrolyte temperature (T) are studied on material removal and Machined depth. A preliminary step is to set up the relations between the coded x - scales and the original scales in which the levels are recorded. In design scale, the lowest and highest values of x are -1.414 and 1.414.

Ranges of voltage and temperatures are taken as :

$$V = 41 - 69$$

$$T = 41^\circ - 69^\circ$$

(a) BOROSILLICATE GLASS

x = -1.414 when V = 41 volts, T = 41 °C

x = 1.414 when V = 69 volts; T = 69 °C

Then, in general,

$$x = a + b * (\text{variable})$$

'a' and 'b' are chosen to satisfy the desired conditions at the ends of the scale.

(i) *Voltage (V):*

$$x = a + b * (V)$$

when x = - 1.414 ; V = 41 volts and -1.414 = a + b * 41

when x = 1.414 ; V = 69 volts and 1.414 = a + b * 69

on solving these two equations simultaneously we get,

a = 5.55

b = 0.101

so,

$$x = -5.55 + 0.101 * V \quad \text{.....(2.4)}$$

Similarly for temperature

$$x = 5.55 + 0.101 * T \text{.....(2.5)}$$

From (2.4) and (2.5) ,voltage and temperature corresponding to level x = -1, 0, 1 are determined. The complete conversion is tabulated in Table 2.2.

Table 2.2 Conversion Table

X	V (volts)	T (^{0}C)
-1.414	41	41
-1	45	45
0	55	55
1	65	65
1.414	69	69

With the above conversions the experiments are conducted in random order according to the plan given in the Table 2.3

Table 2.3 : Plan of Experiments.

Expt. No.	S.No. Acc. to design of exp. (Table 3.1)	Voltage (X_1) (volts)	Temperature(X_2) (^{o}C)
1	5	40	55
2	1	45	45
3	11	55	55
4	3	45	65
5	13	55	55
6	8	55	69
7	2	65	45
8	4	65	65
9	7	55	41
10	6	69	55
11	9	55	55
12	10	55	55
13	12	55	55

(b) ALUMINA

It was found by the trial experiments that the material removal by the ordinary cutting tool was very low, therefore the minimum voltage is increased to 50 volts. Ranges of voltage and temperatures are taken as :

$$V = 50 - 70$$

$$T = 41^{\circ} - 69^{\circ}$$

$x = -1.414$ when $V = 50$ volts, $T = 41^{\circ}$ C

$x = 1.414$ when $V = 70$ volts; $T = 69^{\circ}$ C

Then,

$$x = a + b * (\text{variable})$$

'a' and 'b' are chosen to satisfy the desired conditions at the end of the scale.

(i) *Voltage (V):*

$$x = a + b * (V)$$

when $x = -1.414$; $V = 50$ volts and $-1.414 = a + b * 50$

when $x = 1.414$; $V = 70$ volts and $1.414 = a + b * 70$

on solving these two equations simultaneously we get,

$$a = 5.656$$

$$b = 0.141$$

so,

$$x = -5.656 + 0.141 * V \quad \text{.....(2.6)}$$

Similarly for temperature

$$a = 5.55$$

$$b = 0.101$$

so,

$$x = 5.55 + 0.101 * T \text{.....(2.7)}$$

From (2.6) and (2.7) ,voltage and temperature corresponding to level x = -1, 0, 1 are determined. The complete conversion is tabulated in Table 2.4

Table 2.4 Conversion Table

X	V(volts)	T(^{o}C)
-1.414	70	41
-1	67	45
0	60	55
1	53	65
1.414	50	69

With the above conversions the experiments were conducted in random order according to the plan given in the Table 2.5. Due to the shortage of abrasive cutting tools only two experiments were performed at the zero level.

Table 2.5.: Plan of Experiments.

Expt. No.	Acc. to design of exp. (Table 3.2)	Voltage (X_1) (volts)	Temperature(X_2) (^{o}C)
1	5	50	55
2	1	55	45
3	3	60	41
4	7	55	65
5	11	60	55
6	2	65	45
7	4	65	65
8	6	70	55
9	8	60	69
10	9	60	55

Chapter - 3

Results and Discussion

In this chapter, the effects of supply voltage, and electrolyte temperature on material removal and machined depth are discussed. The discussion is based on experimental results. Two different types of cutting tools were used to ascertain their roles on the mechanism of material removal. They are (A) Ordinary cutting tool (B) Abrasive cutting tool.

3.1 Machining of Borosillicate Glass

CONSTANT MACHINING CONDITIONS USED DURING EXPERIMENTS FOR BOROSILLICATE GLASS :

Tool speed (RPM)	20
Tool Eccentricity	2 mm
Machining time	15 min
Electrolyte concentration	22%by wt

3.1.1 Ordinary Cutting Tool

As discussed in chapter, it was made of mildsteel of the same size and shape as that of the abrasive cutting tool (Fig 2.3).

3.1.1.1 Material removal

From the experimental results (Appendix - D) the following response surface equation is obtained for evaluating material removal (Y_{MR}) by varying supply voltage (x_1) and electrolyte temperature (x_2). *Here, x_1 and x_2 are used as coded level values.*

$$Y_{MR} = 56.214 + 27.532x_1 + 5.556x_2 + 2.450x_1^2 - 2.048x_2^2 + 3.250x_1x_2 \quad \text{.....(3.1)}$$

Using eqn. (3.1), parametric analysis has been conducted as discussed below.

Effect of supply voltage :

Fig. 3.1 shows the effect of supply voltage on material removal at different electrolyte temperature. It is evident that with the increase in supply voltage material removal is also increasing. The reason being that the increase in supply voltage implies increase in discharge energy, hence higher temperature of the workpiece. Beyond a certain voltage, the workpiece showed strong susceptibility towards cracking.

Effect of electrolyte temperature :

The graph relating the electrolyte temperature and material removal at different voltages is shown in Fig. 3.2. It is evident from the graph, that as the electrolyte temperature increases the material removal also increases.

Initially when the electrolyte temperature is increasing material removal is also increasing. An increase in electrolyte temperature increases electrolyte conductivity thus increasing the amount of current. An increase in electrolyte conductivity would mean the accelerated electrolysis process. It would result in a greater rate of evolution of hydrogen gas bubbles at the cathode. The increased rate of formation of gas bubbles at the cathode implies an enhanced rate of sparking hence higher material removal. So it can be said that material removal increases with increased conductivity. The curve shows the decreasing trend after certain temperature depending on the voltage. This is due to the heat losses and debris formed in the electrolyte which cause a decrease in electrolyte conductivity. Due to high temperature, water evaporation increases leading to the electrolyte concentration beyond 22.5 wt percent. The conductivity of NaoH electrolyte beyond 22.5 wt% starts decreasing (Appendix - E). Secondly addition of electrically non-conducting debris also attribute to decrease the electrolyte conductivity. Thus material removal decreases.

3.1.1.2 Machined depth

Machined depth on the work piece is measured with the help of a dial gauge set-up shown in Fig 2.5 . Dial gauge is rigidly fixed on a vertical bar whose one end is fixed with the surface plate. Work piece is kept on the surface plate for measurement of machined depth. The relative vertical displacement of plungerbetween the un machined and machined surface shows the depth achieved on the work piece by this process. The least count of dial gauge is 0.01 mm.

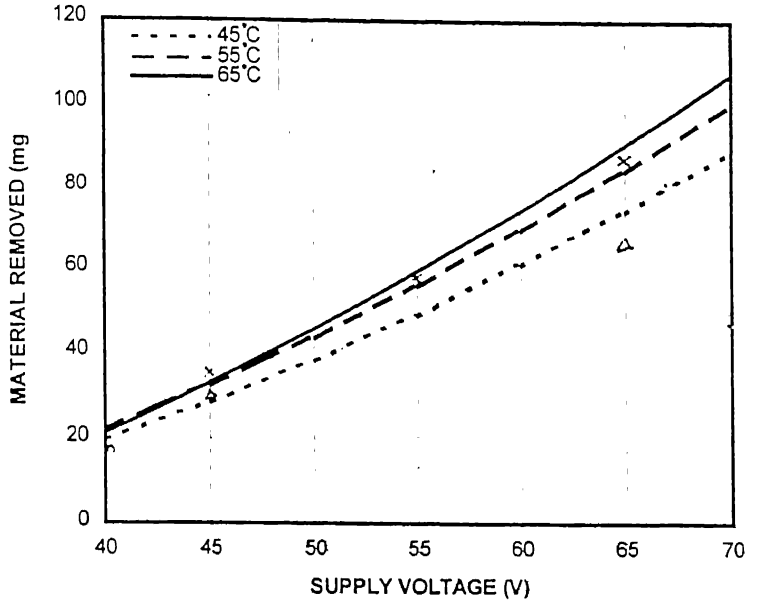

Figure 3.1 : Effect of supply voltage on material removal at different electrolyte temperatures during machining of borosillicate glass
(following symbols indicate various temperatures (°C) as given:
Δ = 45; o = 55; × = 65)

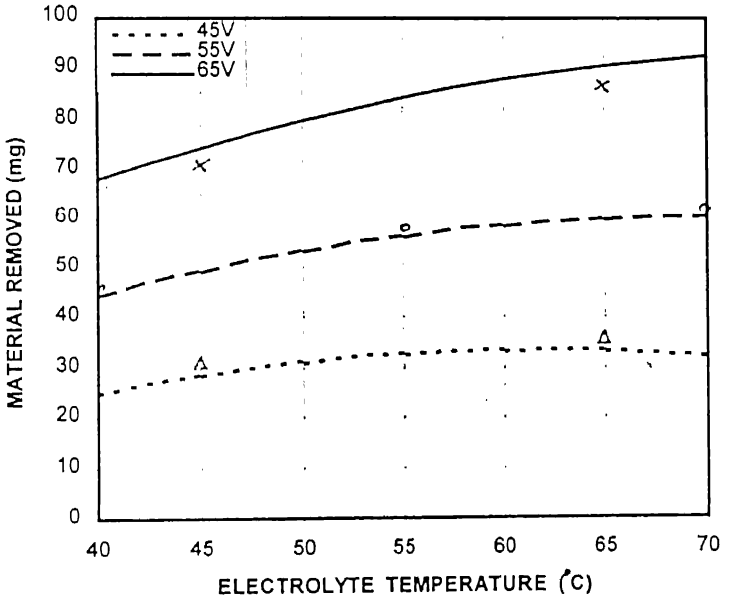

Figure 3.2 : Effect of electrolyte temperature on material removal at different supply voltages during machining of borosillicate glass
(following symbols indicate various voltages (V) as given:
Δ = 45; o = 55; × = 65)

For the machined depth 'Y_{MD}', the response surface equation given below is obtained by calculating the values of constants b_i in eqn (2.2), using the experimental results given in Appendix - D .

$$Y_{MD} = 1.812 + 0.732x_1 + 0.176x_2 - 0.144x_1^2 - 0.068x_2^2 - 0.055x_1x_2 \quad \text{.....(3.2)}$$

Using eqn (3.2), the parametric analysis has been done as discussed below.

Effect of supply voltage :

Fig 3.3 shows the effect of voltage on the machined depth achieved in workpiece material.The nature of the curves are the same as that observed for material removal .It is clear that the effect of voltage is significant on the machined depth achieved.

Effect of electrolyte temperature :

The variation in the machined depth with the variation in the electrolyte temperature at a constant voltage is shown in Fig 3.4. The machined depth also increases with the increase in temperature.

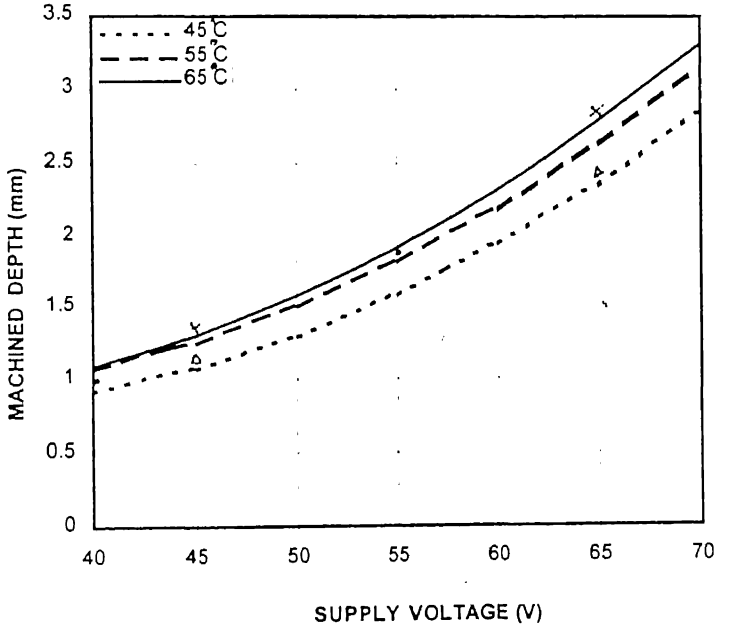

Figure 3.3 : Effect of supply voltage on machined depth at different electrolyte temperatures during machining of borosillicate glass

(following symbols indicate various temperatures (°C) as given:

Δ = 45; o = 55; × = 65)

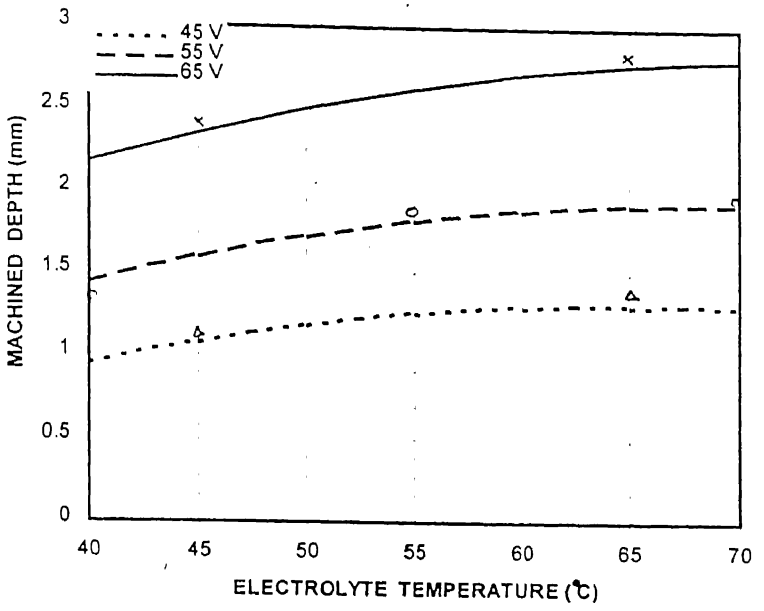

Figure 3.4 : Effect of electrolyte temperature on machined depth at different voltages during machining of borosillicate glass

(following symbols indicate various voltages (V) as given:

$\Delta = 45$; o = 55; × = 65)

3.1.2 Abrasive Cutting Tool

3.1.2.1 Material removal

From the experimental results (Appendix - D) the following response surface equation (3.3) is obtained for evaluating material removal (Y_{MR}) by varying supply voltage (x_1) and electrolyte temperature (x_2). Values of regression coefficients obtained in eqn (3.3) are more than the values of constants obtained in eqn (3.2).

$$Y_{MR} = 60.816 + 32.119x_1 + 5.004x_2 + 8.084x_1^2 - 2.911x_2^2 - 5.500x_1x_2$$

.....(3.3)

Using eqn. (3.3), parametric analysis has been conducted as discussed below.

Effect of supply voltage:

Fig.3.5 shows the effect of supply voltage on material removal at different electrolyte temperature. In this case also we observe the similar trend as in ordinary cutting tool. However, the magnitudes of the material removal is increased. This is due to the combined effect of sparking and abrasive action.

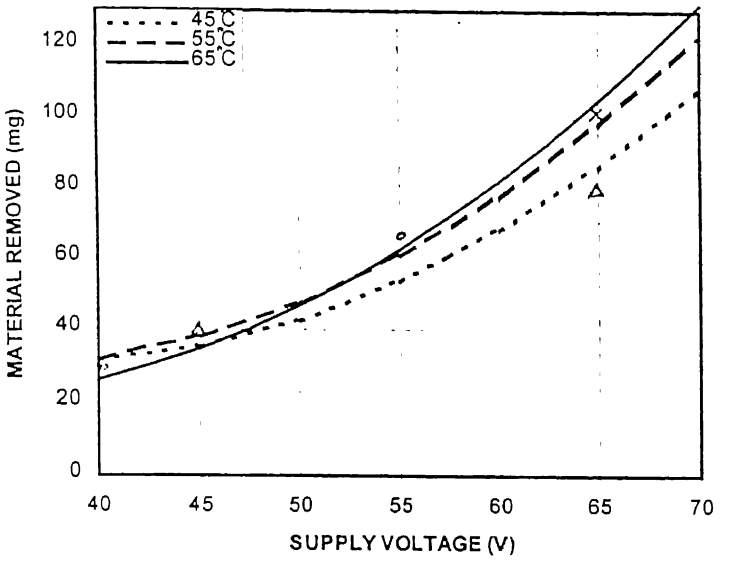

Figure 3.5 : Effect of supply voltage on material removal at different electrolyte temperatures during machining of borosillicate glass
(following symbols indicate various temperatures (°C) as given:
Δ = 45; o = 55; × = 65)

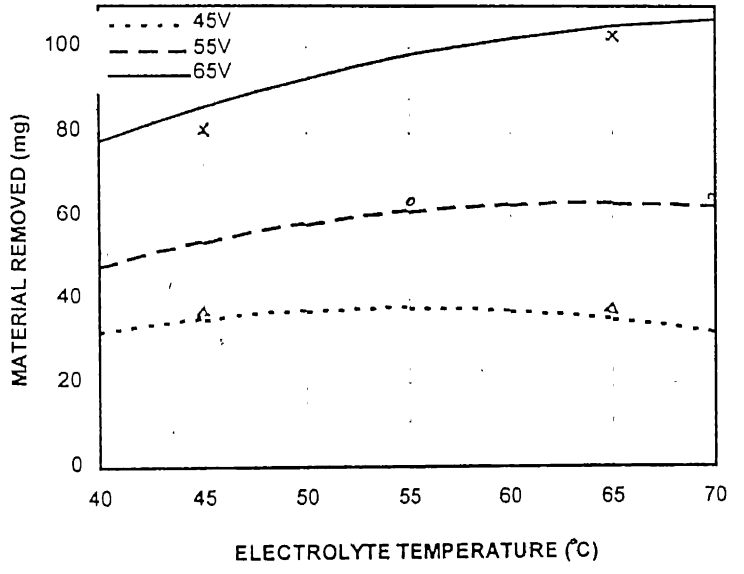

Figure 3.6 : Effect of electrolyte temperature on material removal at different voltages during machining of borosillicate glass
(following symbols indicate various voltages (V) as given:
Δ = 45; o = 55; × = 65)

Effect of electrolyte temperature :

The graph between the electrolyte temperature and material removal at different voltages is shown in Fig. 3.6. It is evident from the graph, that as the electrolyte temperature increases the material removal also increases.

Here also we can observe the same trend as in ordinary cutting tool.. After reaching the optimal point, the decrease in material removal is more in comparison to the ordinary cutting tool. For this behaviour there may be two reasons, as observed during experimentation the electrolyte conductivity and clogging of the abrasive cutting tool. First one has already been explained in 3.1.1.1. Second reason seems to be that after some time of cutting, the sparking does not takes place at some inter spaces in the abrasive tool. This is due to the debris which (debris is non conducting) get clogged in the inter spaces in the cutting tool.

3.1.2.2 Machined depth

For the machined depth 'Y_{MD}', the response surface equation given below is obtained by calculating the values of constants b_i , using the experimental results given in Appendix - D.

$$Y_{MD} = 2.040515 + 0.699623x_1 + 0.203208x_2 - 0.190170x_1^2 - 0.05475x_2^2 - 0.0975x_1x_2 \quad \text{.....(3.4)}$$

Using eqn (3.4), the parametric analysis has been done as discussed below.

Effect of supply voltage :

Fig 3.7 shows the variation in machined depth obtained with the variation in supply voltage at constant temperature. The trend is the same as in case of ordinary cutting tool (Fig 3.3).

Effect of electrolyte temperature :

The nature of curves showing (Fig 3.8) the effect of electrolyte temperature on machined depth achieved in workpiece material is the same as that obtained for ordinary cutting tool (Fig 3.4).

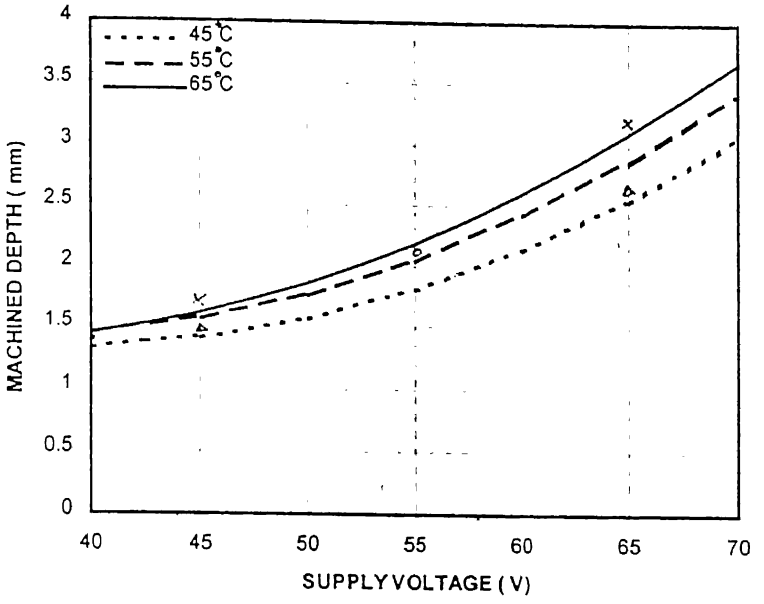

Figure 3.7 : Effect of voltage on machined depth at different temperatures during machining of borosillicate glass

(following symbols indicate various temperatures (℃) as given:

Δ = 45; o = 55; × = 65)

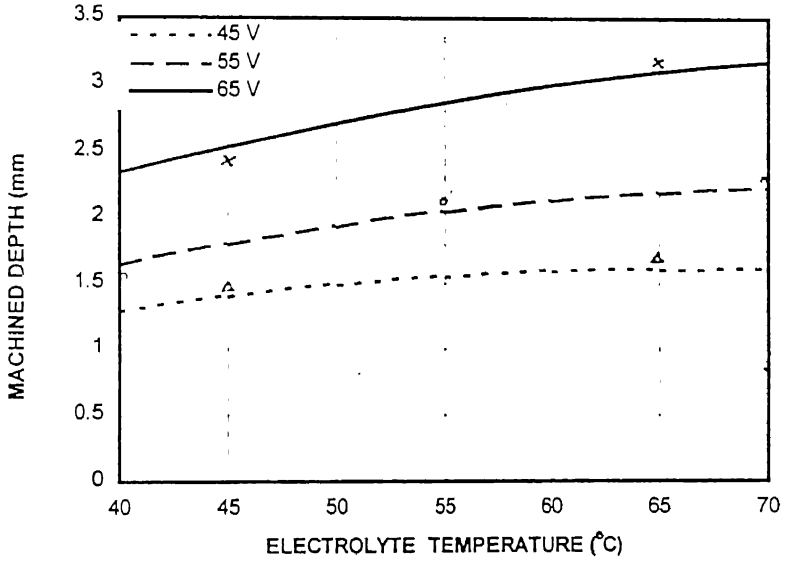

Figure 3.8 : Effect of temperature on machined depth at different voltages during machining of borosillicate glass

(following symbols indicate various voltages (V) as given :

Δ = 45; o = 55; × = 65)

3.1.3 Comparison of Ordinary and Abrasive Cutting Tools

3.1.3.1 Material removal

Fig 3.9 shows the comparison of material removal obtained by the (O C T) and the abrasive cutting tool (ACT) at 55 °C temperature at different voltages. It is clearly visible that material removal has increased with the abrasive cutting tool while machining under the same conditions. It would be possible to increase the material removal further at the same working conditions by increasing the feed rate. In that case good circular accuracy can't be achieved. It is similar to drilling where by increasing feed rate, the material removal increases. The reason is as follows.

Feed rate is decided by glowing of the bulb (as discussed in sec 2.4). If glowing of the bulb stops, the feed rate is increased, else it is not disturbed. If the feed rate increases beyond this value, workpiece fixture starts vibrating and also this increased feed rate does not allow the cutting tool to rotate in exact trepaning path. This would cause non-circularity of the hole. This may be explained on the basis of partial penetration of the tool tip in the work piece. Because of partial penetration, it tries to mechanically cut the material from the w/p. Fig 3.10 shows the comparison of material removal obtained by the OCT and the ACT at 55 voltage at different temperatures.

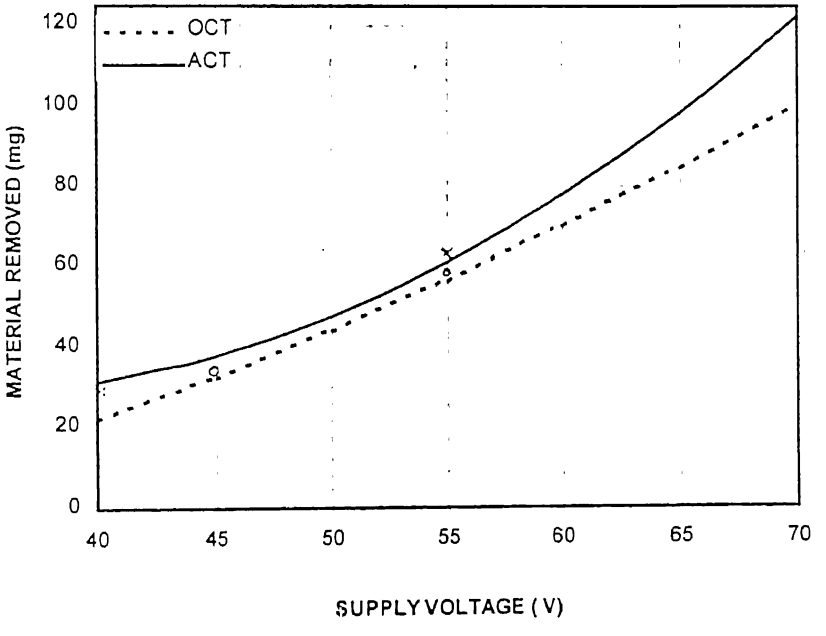

Figure 3.9 : Effect of supply voltage on material removal during machining of borosillicate glass with different cutting tools, at 55 °C electrolyte temperature (following symbols indicate various cutting tools as given: o = OCT; × = ACT)

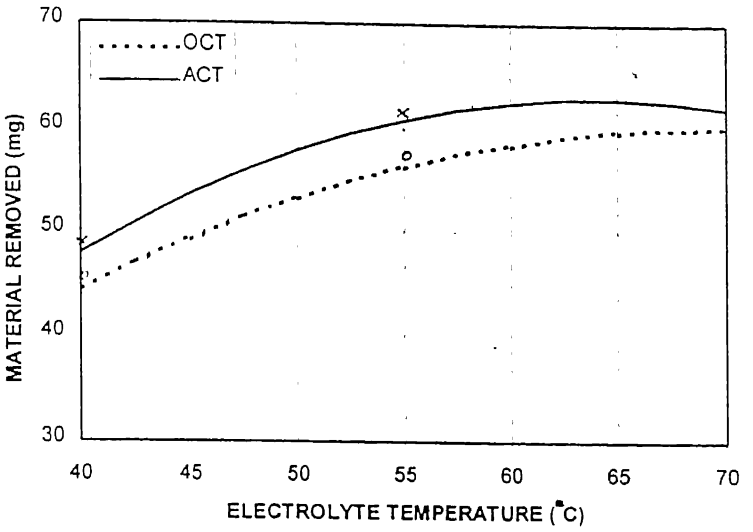

Figure 3.10 : Effect of electrolyte temperature on material removal during machining of borosillicate glass with different cutting tools at 55 V
(following symbols indicate various cutting tools as given:
o = OCT; × = ACT)

3.1.3.2 Machined depth

Fig 3.11 shows the comparison of machined depth obtained by the ordinary cutting tool and the abrasive cutting tool at 55 °C temperature at different voltages. It is clearly visible that material removal has increased with the abrasive cutting tool while machining under the same conditions. Fig 3.12 shows the comparison of machined depth obtained by the ordinary cutting tool and the abrasive cutting tool at 55 voltage at different temperatures.

3.2 Machining of Alumina

CONSTANT MACHINING CONDITIONS DURING EXPERIMENT WITH ALUMINA :

Tool speed (RPM)	20
Tool Eccentricity	1mm
Machining time	30 min
Electrolyte concentration	22%by wt

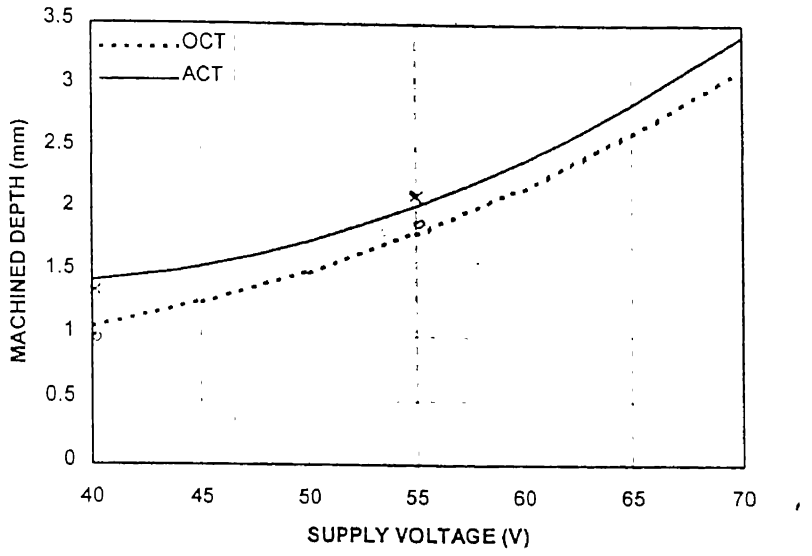

Figure3.11 : Effect of supply voltage on machined depth during machining of borosillicate glass with different cutting tools, at an electrolyte temperature of 55 °C. (following symbols indicate various cutting tools as given:

o = OCT; × = ACT)

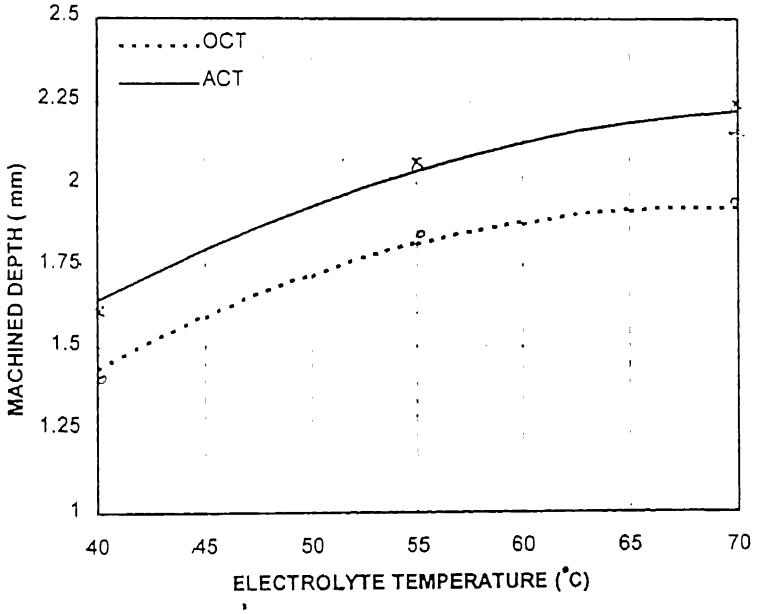

Figure 3.12 : Effect of electrolyte temperature on machined depth during machining of borosillicate glass with different cutting tools at 55 V.

(following symbols indicate various cutting tools as given:

o = OCT; × = ACT)

3.2.1 Ordinary Cutting Tool

As discussed in chapter 2, it was made of mildsteel of the same size and shape as the abrasive cutting tool (Fig 2.3).

3.2.1.1 Material removal

From the experimental results (Appendix - D) the following response surface equation is obtained for evaluating material removal (Y_{MR}) by varying supply voltage (x_1) and electrolyte temperature (x_2).

$$Y_{MR} = 7.500 + 3.423x_1 + 0.8019x_2 + 1.0625x_1^2 - 0.9375x_2^2 + 0.750x_1x_2 \quad \text{.....(3.5)}$$

Here it is to be noted that the signs of the constants in this eqn and that in eq (3.1) are the same. However the magnitudes are quite different. Using eqn. (3.5), parametric analysis has been conducted as discussed below.

Effect of supply voltage:

Fig. 3.13 shows the effect of supply voltage on material removal at different electrolyte temperatures. Curves show the increasing trend, i.e the material removal increases with increase in voltage. Hardness of the alumina is more than the glass. Therefore, material removal is observed to be lower than that in case of borosillicate glass.

Effect of electrolyte temperature:

The graph between the electrolyte temperature and material removal at different voltages is shown in Fig.3.14. It is evident from the graph, that as the electrolyte temperature increases the material removal also increases.

3.2.1.2 Machined depth

For machined depth ' Y_{MD} ', the response surface equation given below is obtained by calculating the values of constants b_i in eqn (2.2), using the experimental results given in Appendix - D.

$$Y_{MD} = 0.065 + 0.068x_1 + 0.007x_2 + 0.042x_1^2 - 0.003x_2^2 - 0.0025x_1x_2$$

.....(3.6)

Using eqn (3.6), the parametric analysis has been done as discussed below.

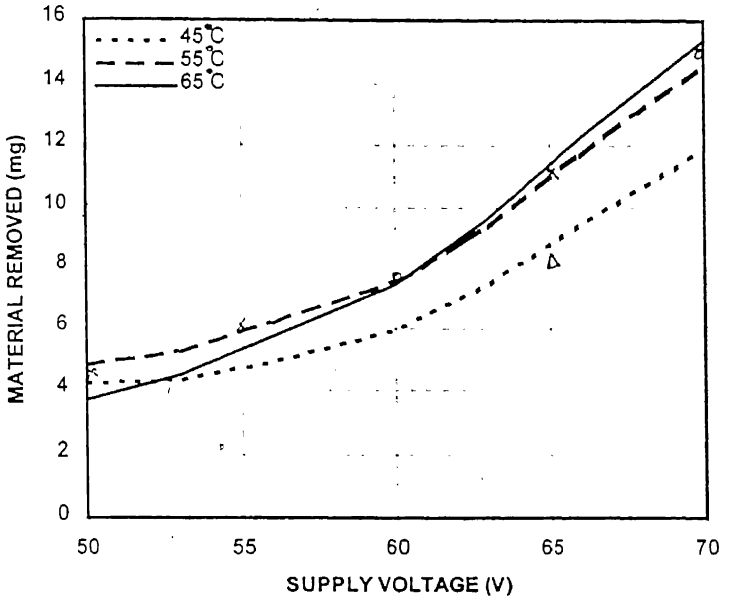

Figure 3.13 : Effect of voltage on material removed at different temperatures during machining of alumina.

(following symbols indicate various temperatures (°C) as given:

Δ = 45; o = 55; × = 65)

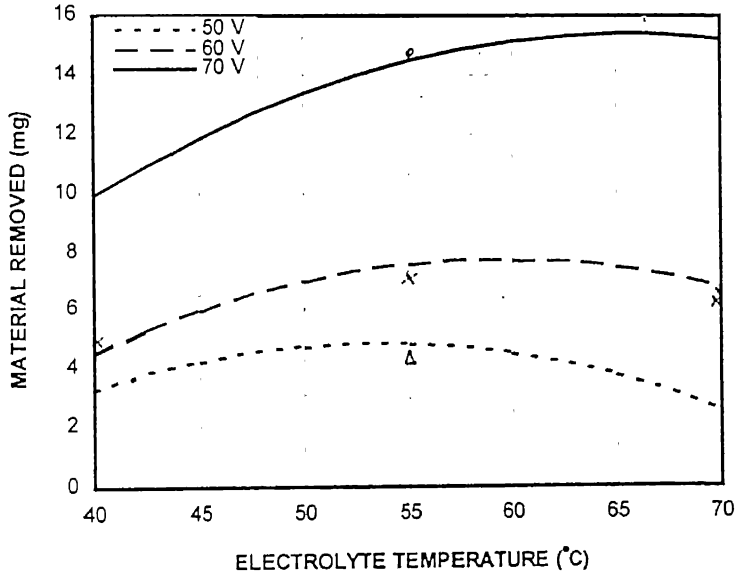

. Figure 3.14 : Effect of temperature on material removal at different voltages during machining of alumina.

(following symbols indicate various voltages(V) as given:

Δ = 50; o = 60; × = 70)

Effect of supply voltage:

It is evident from the graph Fig 3.15 that the machined depth increases with increase in the electrolyte temperature at constant voltage. In this case, the effect of electrolyte temperature on machined depth is not so significant as in case of borosillicate glass.

Effect of electrolyte temperature:

The nature of curves showing (Fig 3.16) the effect of electrolyte temperature on machined depth achieved in workpiece material is similar as that obtained for machined depth with OCT (Fig 3.4). However the magnitudes in these two cases are different.

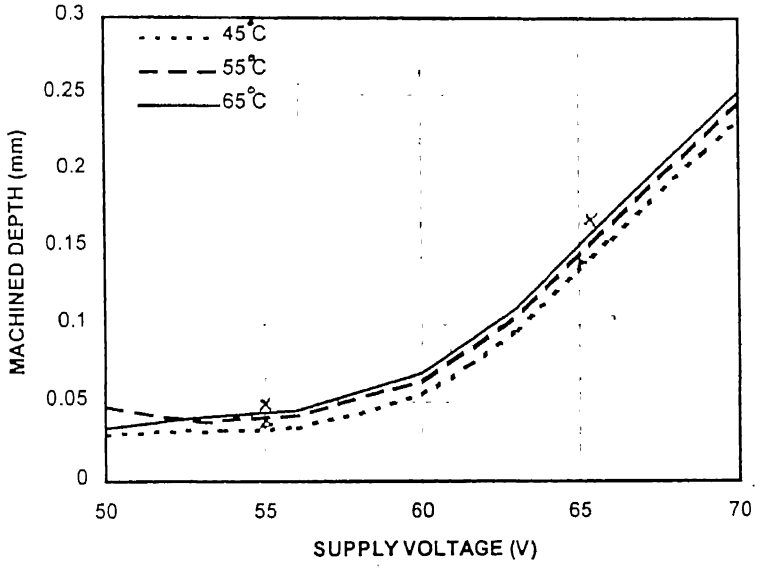

Figure 3.15 : Effect of voltage on machined depth at different temperatures during machining of alumina

(following symbols indicate various temperatures (°C) as given:

$\Delta = 45$; $o = 55$; $\times = 65$)

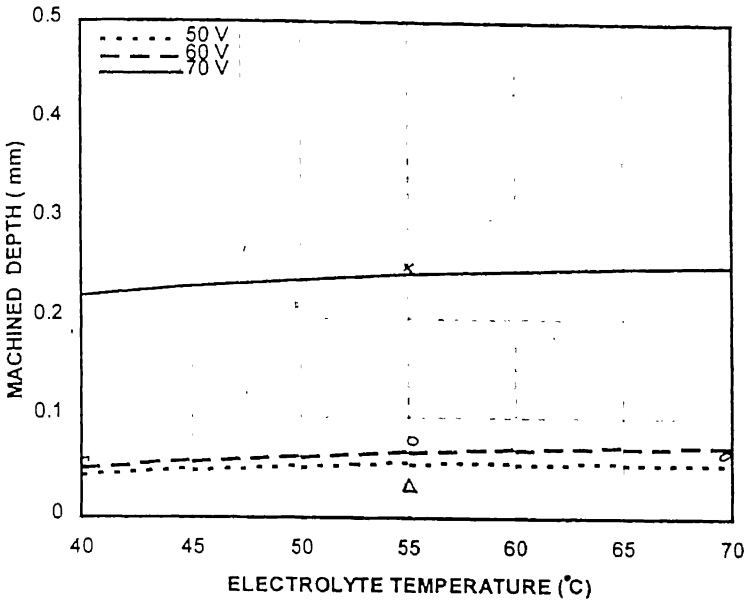

Figure 3.16 : Effect of temperature on machined depth at different voltages during machining of alumina

(following symbols indicate various voltages as given:

$\Delta = 50$; o = 60; × = 70)

3.2.2 Abrasive Cutting Tool

3.2.2.1 Material removal

From the experimental results (Appendix - D) the following response surface equation is obtained for evaluating material removal (Y_{MR}) by varying supply voltage (x_1) and electrolyte temperature (x_2)

$$Y_{MR} = 14.5 + 3.6x_1 + 1.1554x_2 - 0.625x_1^2 - 1.875x_2^2 - 0.25x_1x_2$$

.....(3.7)

Using eqn. (3.7), parametric analysis has been conducted as discussed below

Effect of supply voltage :

Fig. 3.17 shows the effect of supply voltage on material removal at different electrolyte temperature. The material removal with increase in voltage is increased. This is due to the sparking action assisted by the abrasive action.

Effect of electrolyte Temperature :

The graph between the electrolyte temperature and material removal at different voltages is shown in Fig.3.18. It is evident from the graph, that as the electrolyte temperature increases the material removal also increases. The decrease in material removal after attaining the maxima is attributed to the same as discussed earlier in case of borosillicate glass.

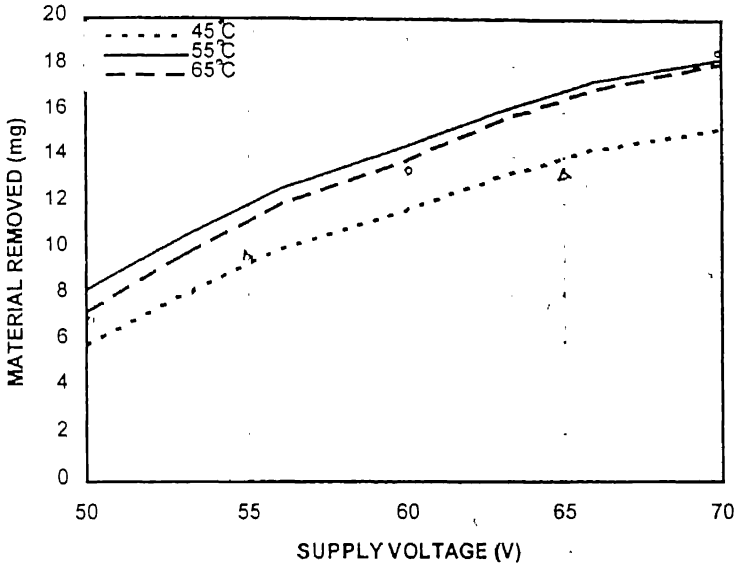

Figure 3.17 : Effect of voltage on machined depth at different temperatures during machining of alumina

(following symbols indicate various temperatures (℃) as given:

$\Delta = 45$; $o = 55$; $\times = 65$)

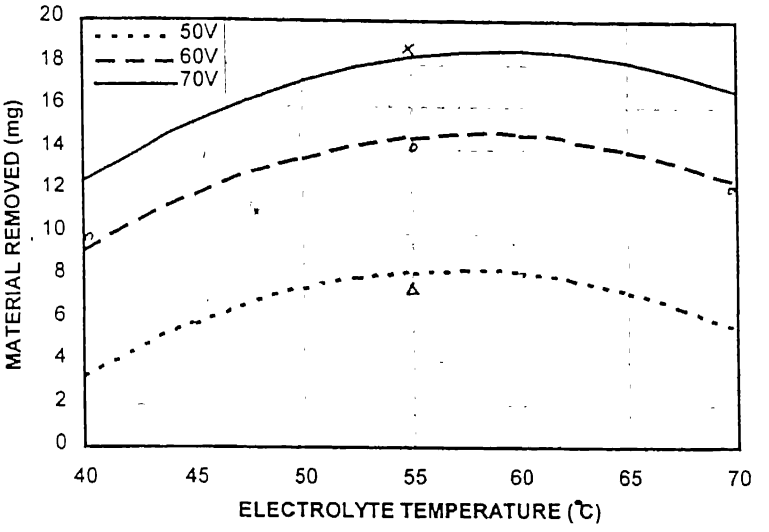

Figure 3.18 : Effect of temperature on machined depth at different temperatures during machining of alumina

(following symbols indicate various voltages as given:

$\Delta = 50$; $o = 60$; $\times = 70$)

3.2.2.2 Machined depth

For machined depth 'Y_{MD}', the response surface equation given below is obtained by calculating the values of constants b_i in eq (2.2) , using the experimental results given in Appendix - D.

$$Y_{MD} = 0.255 + 0.127x_1 + 0.024x_2 + 0.023x_1^2 + 0.010x_2^2 - 0.013x_1x_2$$

.....(3.8)

Using eqn (3.8), the parametric analysis has been carried out as discussed below.

Effect of supply voltage:

The nature of curves (Fig 3.19) shows the effect of voltage on the machined depth achieved in the workpiece.

Effect of electrolyte temperature :

The nature of curves (Fig 3.20) shows the effect of electrolyte temperature on machined depth achieved in workpiece.

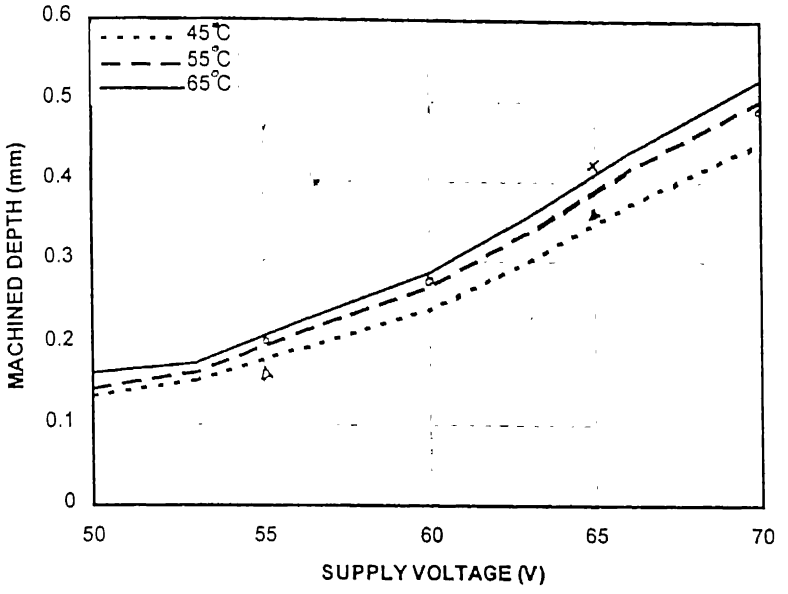

Figure 3.19 : Effect of voltage on machined depth at different temperatures during machining of alumina

(following symbols indicate various temperatures (°C) as given:

Δ =45; o=55; ×=65)

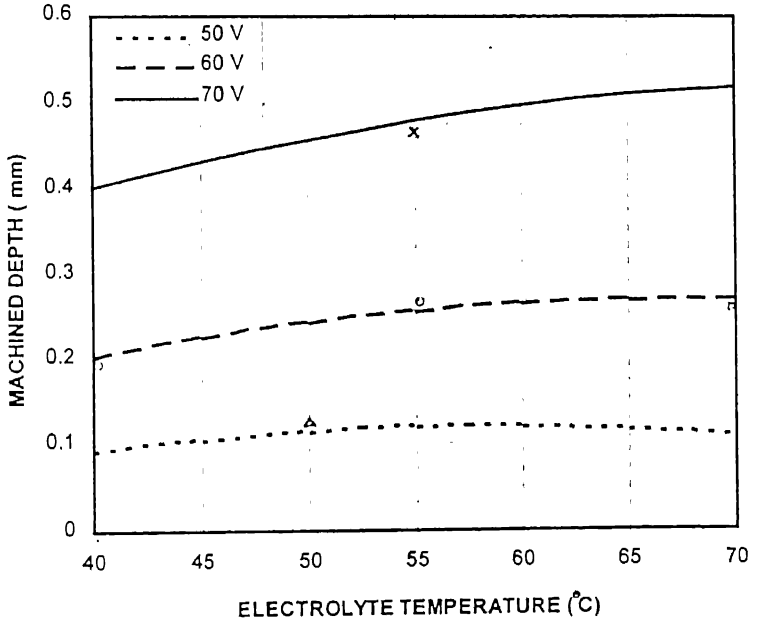

Figure 3.20 : Effect of Electrolyte temperature on machined depth at different voltages during machining of alumina.

(following symbols indicate various voltages (V) as given:

Δ = 50; o = 60; × = 70)

3.2.3 Comparison of Ordinary and Abrasive Cutting Tools

3.2.3.1 Material removal

The graph (Fig 3.21) shows that the material removal is higher for the ACT as compared to OCT under the same machining conditions. Fig 3.21 shows a comparison of the performance of the ordinary cutting tool and abrasive cutting tool at 55^0C at different voltages. Fig 3.22 shows a comparison of the performance of the ordinary cutting tool and abrasive cutting tool at 60 V at different temperatures.

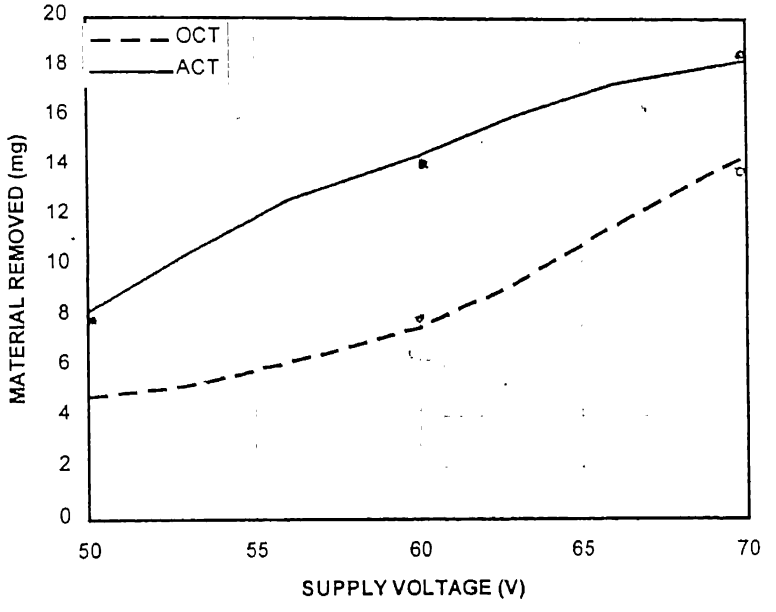

Figure 3.21 : Effect of supply voltage on material removal during machining of alumina with different cutting tools at 55 °C

(following symbols indicate various cutting tools as given:

o = OCT; ⊗ = ACT)

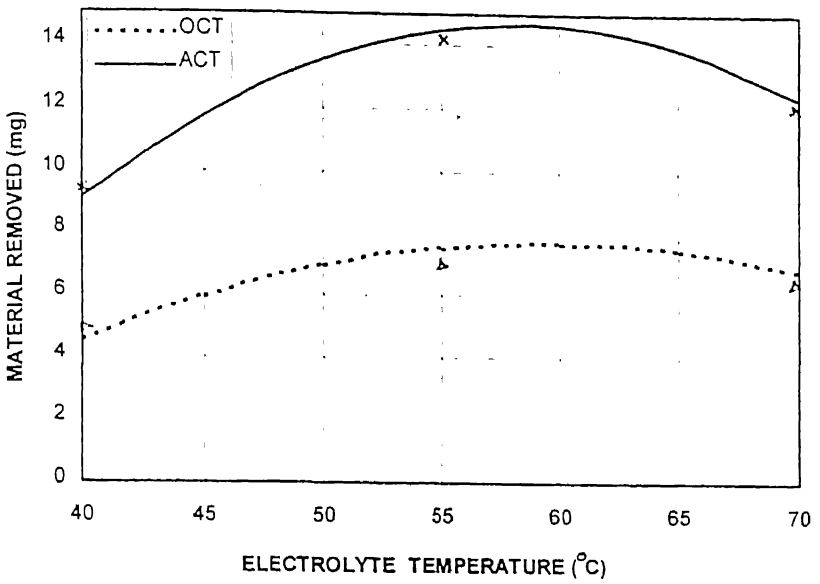

Figure 3.22 : Effect of electrolyte temperature on material removal during machining of alumina with different cutting tools at 60 (V).
(following symbols indicate various cutting tools as given:
o = OCT; × = ACT)

3.2.3.2 Machined depth

The graph (Fig 3.23) shows that the machined depth is higher for the abrasive cutting tool as compared to ordinary cutting tool under the same machining conditions. Fig 3.23 shows a comparison of the performance of the ordinary cutting tool and abrasive cutting tool at 55^0C at different voltages. Fig 3.24 shows a comparison of the performance of the ordinary cutting tool and abrasive cutting tool at 60V at different temperatures

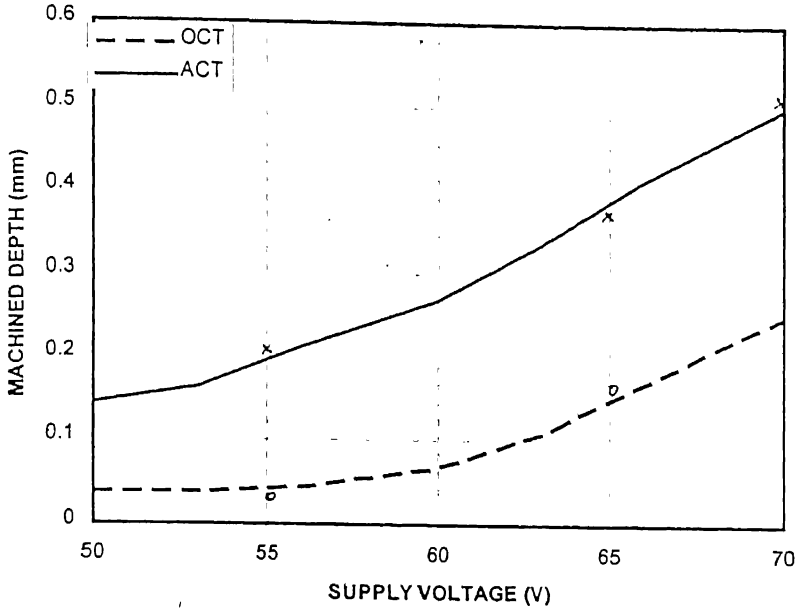

Figure 3.23 : Effect of supply voltage on machined depth during machining of alumina with different cutting tools at 55 °C

(following symbols indicate various cutting tools as given:

o = OCT; × = ACT)

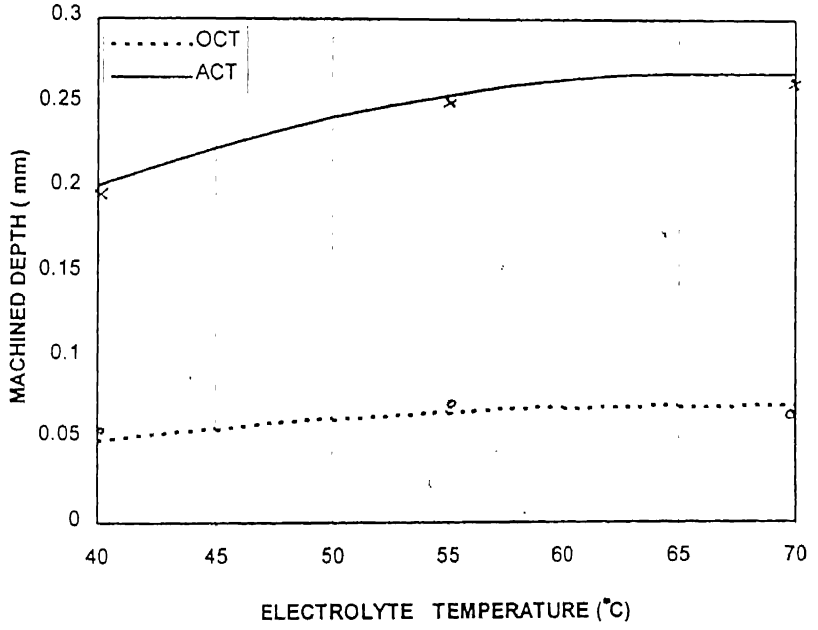

Figure 3.24 : Effect of Electrolyte temperature on machined depth during machining of alumina with different cutting tools at 60 V

(following symbols indicate various cutting tools as given:

o = OCT; × = ACT)

3.3 Comparison of Process Performance for both meterials

Fig 3.25 and Fig 3.26 show comparison of material removal of the glass and alumina with different cutting tools. Fig 3.27 and Fig 3.28 show coparison of machined depth of BSG and alumina with different cutting tools. It is clearly visible that material removal and machined depth are more for BSG when compared to alumina. It also clearly visible that performance with ACT is better than OCT for both the materials.

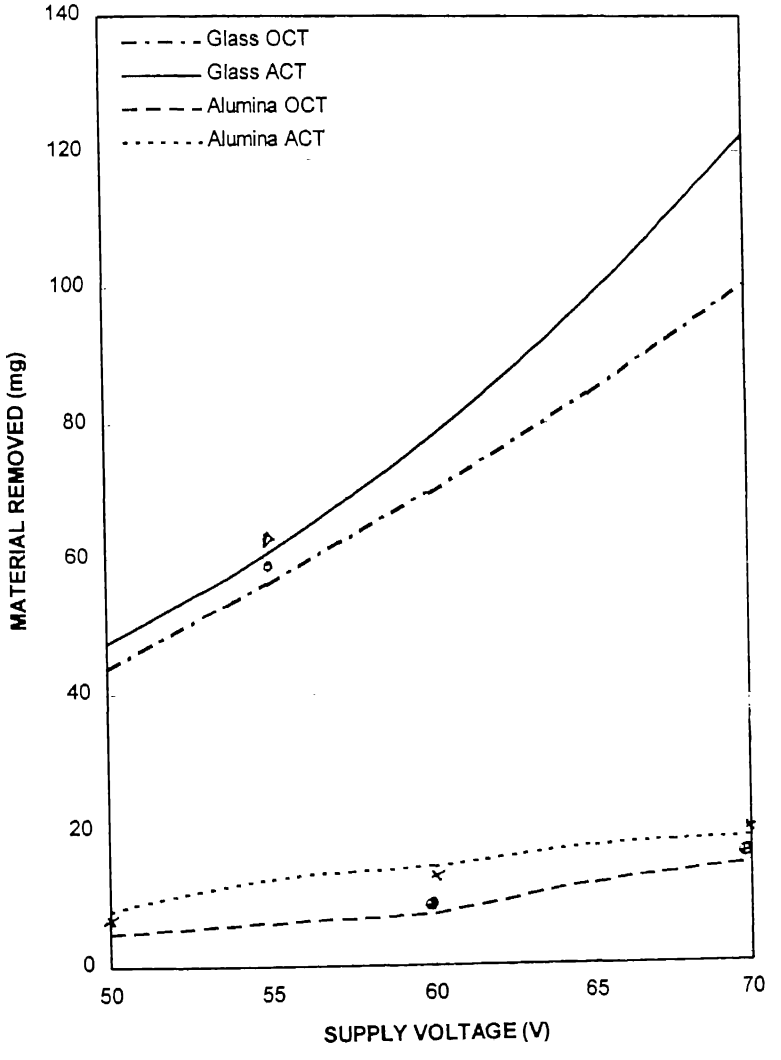

Voltage (V)	Alumina % of improvement with ACT	BSG % of improvement with ACT
50	70	8
55	106	8
60	93	11
65	49	53
70	27	22

Figure 3.25 : Effect of supply voltage on material removal of alumina and glass with different cutting tools at 55 °C

(following symbols indicate various cutting tools as given :

Δ = Glass (ACT); o = Glass (OCT); × = Alumina (ACT); ⊕ = Alumina (OCT))

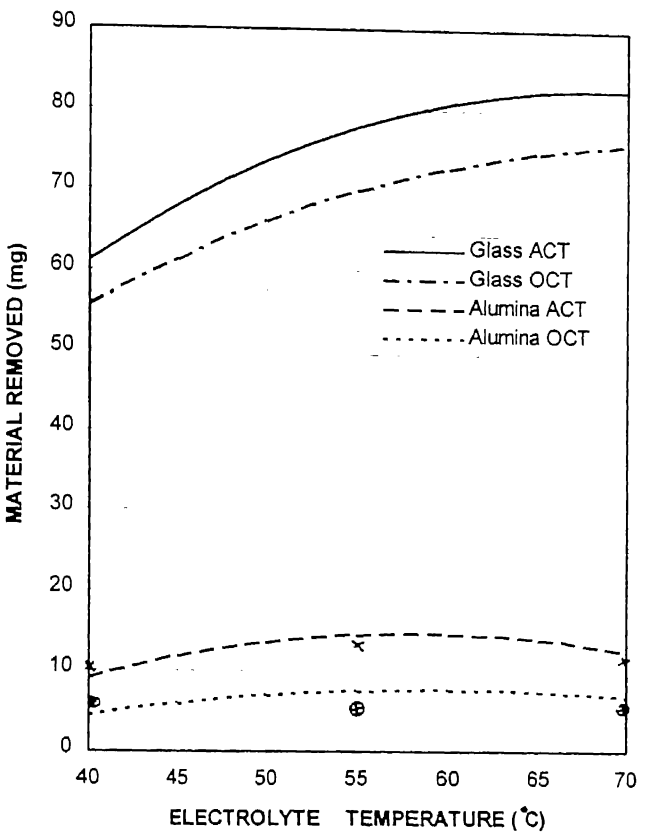

Temperature (°C)	Alumina % of improvement with ACT	BSG % of improvement with ACT
40	102	10
45	97	11
50	95	11
55	99	11
60	91	8
65	87	7
70	83	9

Figure 3.26 : Effect of electrolyte temperature on material removal of alumina and glass with different cutting tools at 60 V

(following symbols indicate various cutting tools as given:

Δ = glass (ACT); o = Glass (OCT); $\times$ = Alumina (ACT); $\oplus$ = Alumina (OCT))

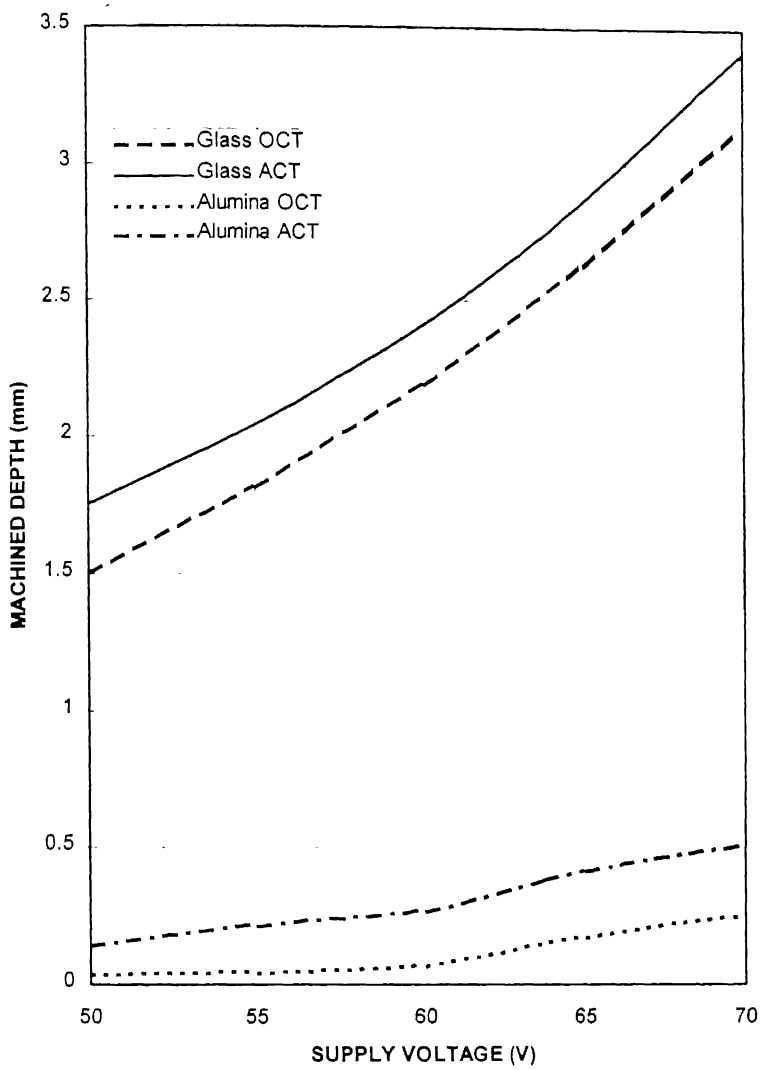

Voltage (V)	Alumina % of improvement with ACT	BSG % of improvement with ACT
50	276	18
55	388	12
60	306	10
65	144	8
70	102	8

Figure 3.27 : Effect of supply voltage on machined depth of alumina and glass with different cutting tools at 60 °C

(following symbols indicate various cutting tools as given:

Δ = glass (ACT); o = Glass (OCT); × = Alumina (ACT); ⊕ = Alumina (OCT))

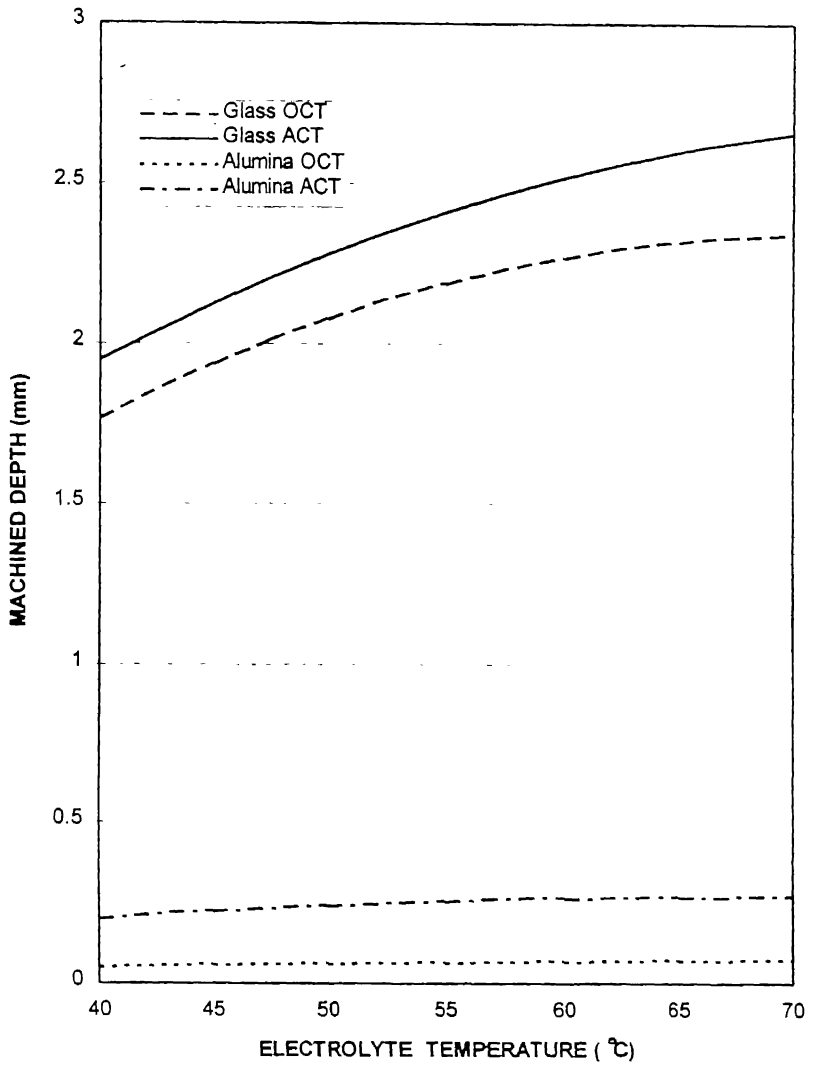

Temperature (°C)	Alumina % of improvement with ACT	BSG % of improvement with ACT
40	320	10
45	305	9
50	301	10
55	296	10
60	281	11

Figure 3.28 : Effect of electrolyte temperature on machined depth of alumina and glass with different cutting tools at 60 V

(following symbols indicate various cutting tools as given:

Δ = glass (ACT); o = Glass (OCT); $\times$ = Alumina (ACT); $\oplus$ = Alumina (OCT))

3.4 S E M Analysis

3.4.1 Study of machined profile

Various photographs of machined profiles and machined surfaces, were taken by the scanning electron microscope (SEM). Before scanning the machined surface by SEM, it was vaccum coated with an alloy of gold (90 %) and platinum (10%) to make the machined surface conducting. Fig 3.29 shows the machined profiles of different samples by SEM. Here our aim is to show the machined surface appearance in alumina and BSG with ACT (Fig 3.29 (a) (c) (d) (e)) and OCT (Fig 3.29 (b) (f)).

Fig 3.29 (a) shows a clear view of through hole machined in BSG with ACT. Fig 3.29 (b) and (c) show the same with OCT and ACT respectively. Fig 3.29 (d) shows clearly the grinding marks on the machined surface of alumina at low voltage of 55 V. Where UMD is the unmachined region. MD is machined region. Fig 3.29 (e) also shows the the grinding marks at higher magnification. Fig 3.29 (f) shows the machined region for alumina with OCT. It is to be noted here that there are no grinding marks.

3.4.2 Study of used cutting tools

Our aim of cutting tool analysis is to find evidence for the pull out of abrasives on the cylindrical surface and at the bottom surface of the cutting tool. We couldn't found the same on the cylindrical surface of ACT. Fig 3.30 (a) and (b) show the used cutting tool at 70 V. The whitish region indicates the core material of the cutting tool. It gives an idea of pull out of abrasives at the bottom of the cutting tool. Secondly we tried to find out clogging of the cutting tool .We have not succeeded. Fig 3.30 (c) and (d) shows the clear view of abrasive cutting tools.

(a) Through hole by trepanning in BSG at 60 V with ACT

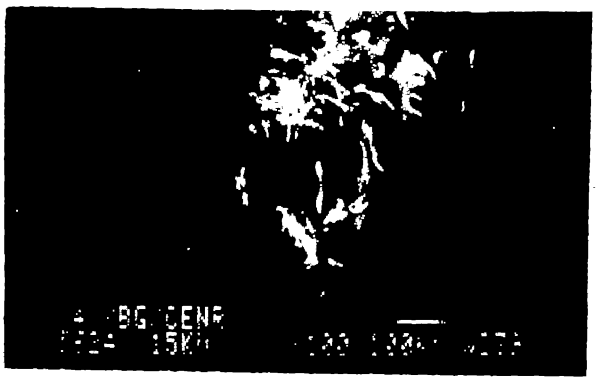

(b) Part of the side surface of BSG machined at 60 V with OCT

(c) Enlarged view of (a) showing side surface of the hole.

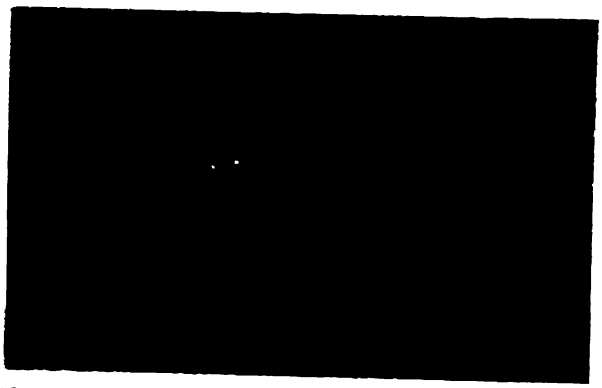

(d) Blind hole machined in alumina at 55 V with ACT

e) Enlarged view of (d) in alumina at 55 V with ACT

(f) Blind hole machined in alumina at 70 V WITH OCT

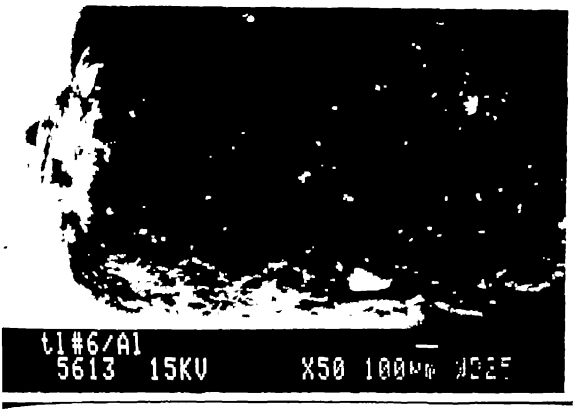

(a) Used ACT on alumina at 70 V.

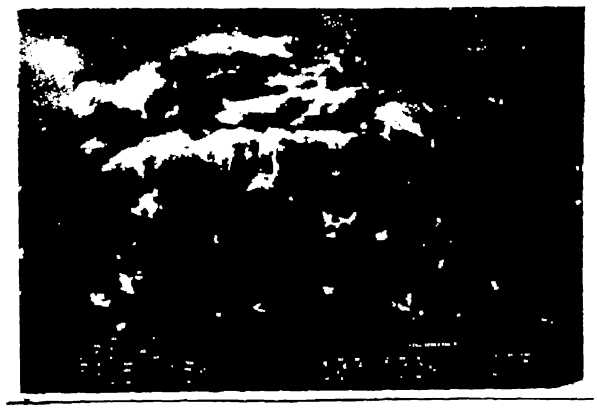

(b) Enlarged view of (a) ACT on alumina at 70 V.

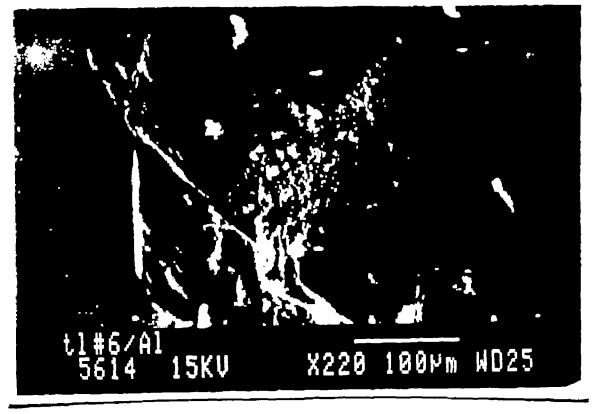

(c) A clear View of the abrasive cutting tool used at 70 V on alumina

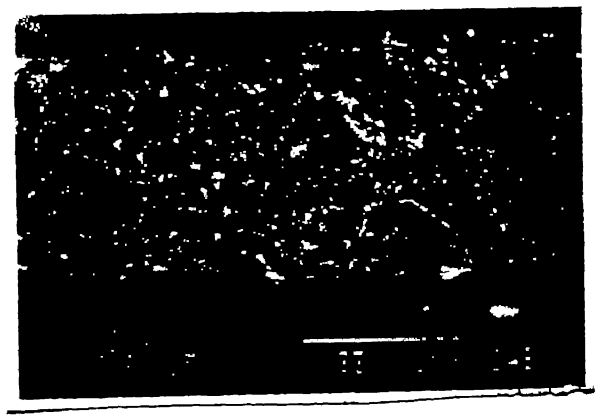

(d) Enlarged view of the ACT at 50 V on alumina

Figure 3.30 : SEM study of used cutting tools in ECSM process

Chapter-4

Conclusions and Scope for Future Work

4.1 Conclusions

From the present work the following conclusions have been made :

1. Electrochemical Spark machining with abrasive cutting tools has shown the improved performance (material removal and machined depth) related to machining of electrically non conducting materials viz. alumina and borosillicate glass.
2. The improvement in the machining performance of ECSM process with the abrasive cutting tools vanishes beyond a certain temperature of the eletrolyte.
3. At high voltages glass specimens have shown succepatability towards cracking.

4.2 Scope for the future work

1. Pulsed power supply with the pulse time of the order of microsecond can be used for increasing the material removal rate and improving surface finish.
2. Use of combination of Electrolyte for the ECSM process is still an open field for research.

REFERENCES

1. Jain V. K., Gautam N -"Experimental investigations into ECSD process using various tool kinematics", Int J. Mach Tools Manufact. 38, pp. 15-27 1998.
2. Basak., Ghosh A., - "Mechanism of spark generation during ECSM", Journal of Material Processing Technology, 62, pp. 46-53, 1996.
3. Manoj singh. -"Effect of porosity and glass content on machining of alumina ceramics by ECSM ", M . Tech Thesis ; IIT KANPUR 1997.
4. T. Suchiya, T. Inoue, and M. Miyazki-"Wire electrochemical discharge machining of glasses and ceramics", Proceedings of 5 th International Conference on Production Engineering, Tokyo pp. 413-417, 1984.
5. Crichton I. M., McGrough J.A.-"Studies of discharge mechanism in electrochemical arc machining", Journal of applied Electrochemistry, 15, pp. 113-119, 1985.
6. Jain V.K., P. Srinivasa, Choudhary S. K., Rajurkar K. P.-"Experimental investigation into travelling wire ECSM of composites", Trans. of ASME, Journal of Engineering for Industry, 113, pp. 75-84, 1991.
7. Allesu K., Umesh Kumar N., Muju M. K., Ghosh A. - "Some investigations into spark machining of nonconductiong materials", 12 th AIMTDR Conference, IIT Delhi pp. 521-524, 1986.
8. Singh Y.P., Jain V.K., Prashant kumar, Agrawal D.C.-"Design and fabrication of TW-ECSM and machining PZT ceramics", Material Processing Technology, vol 58, pp. 24-31, 1996.
9. Nesarikar V.V., Jain V.K., Chaudhury S.K. -"Travelling Wire Electrochemical Spark Machining of Thick sheets of Kaevlar-Epoxy Composites", Proc.of 16th AIMTDR Conf., pp. 672-677, 1994.

10. Raghuram V., Pramila T., Srinivasa Y.G., Narayanswamy K.,-"Effect of circuit parameters on the electrolytes in the Electrochemical discharge phenomenon". Journal of Materials Processing Technology, 52, pp. 289-300, 1995.

11. Chak S.K.-"Electrochemical spark machining of Alumina and Quartz", M.Tech Thesis ; IIT KANPUR 1996.

12. William G. Cochran, and Gertrude M. Cox, "Experimental Designs", Asia Publishing House, Bombay, pp. 334-353, 1977.

13. Ryshkewitch E - "Oxide ceramics", Academic Press, New York, 1960

14. From the manual of manufacturers of BSG.

Appendix - A

Borosillicate glass

SiO_2	B_2O_3	Al_2O_3	Na_2O_3
81%	13%	2%	4%

Table A.1 : Chemical composition of borosilicate glass [14]

Softening point	820°C
coefficient of thermal expansion	$32.5X10^{-6}$ / K
conductivity	1.1304 W / m K

Table A.2 : Physical properties of borosilicate glass [14]

Appendix-B

Alumina

Melting Point	2050 + 5 C
Coefficient of thermal expansion	2 X 10^{-1} / K
Thermal conductivity	0.0723 cal / c cm sec

Table B.1 : Physical properties of Alumina [13]

Material	N/mm^2
Aluminium oxide	20000 - 30000
Cubic boron nitride	50000
Diamond	70000 -80000

Table B.2 : Hardness of abrasive materials [13]

Appendix-C

Following code is a program to find out the regression coefficients for Abrasive material removal. Similarly constants were found for the machined depth also.

$A_{[10X6]}$ = Coefficient matrix

$B_{[10X1]}$ = Response Matrix

$X_{[6X1]}$ = Regression constants(to be found) matrix

$$A X = B \quad \text{.....(1)}$$

For solving Eq (1) A should be square matrix, here A is a rectangular Matrix. To convert A into square matrix. Eq (1) is pre multiplied by A^T on both sides.

Thus Eq (1) becomes

$$A^T A X = A^T B$$

$$X_{[6X1]} = [A^T A]^{-1}_{[6X6]} \; A^T_{[6X10]} \; B_{[10X1]} \quad \text{.....(2)}$$

(2) has been transformed into the following code as input file. Using Mat lab Eq (2) has been solved.

```
A =[1 -1 -1 1 1 1;1 1 -1 -1 1 1;1 -1 1 -1 1 1;1 1 1 1 1 1;1 -1.414 0 0 2 0;1 1.414 0 0 2
0;1  0 -1.414 0 0 2;1 0 1.414 0 0 2;1 0 0 0 0 0;1 0 0 0 0 0]

B =[9 13 11 16 06 20 09 12 14 15]

b = (A') * A

c = inv  (b)          (Here b, c, d are the temporary matrices)

d = c* (A')

X= d * B'
```

Appendix-D

Table D.1: Experimental results for borosillicate glass

o.n.	R.No.	Voltage (Volts)	Temperature (°C)	Average Conductivity (mmho/cm) (t)	Initial weight (g) w_1	Final weight (g) w_2	M.R. w_1-w_2 (g)	Machine depth (mm)	Feed(mm/min.)
1	1	45	45	475(0) 470(7) 474(15)	2.645	2.614	0.031	1.16	0.0955
	1A	45	45	475(0) 469(7) 472(15)	2.261	2.221	0.040	1.49	0.109
2	5	40	55	521(0) 513(7) 517(15)	1.383	1.366	0.017	0.96	0.0855
	5A	40	55	519(0) 511(7) 514(15)	1.944	1.920	0.024	1.34	0.0955
3	11	55	55	514(0) 509(7) 512(15)	2.045	1.988	0.057	1.93	0.156
	11A	55	55	511(0) 507(7) 510(15)	2.482	2.418	0.064	2.17	0.169
4	3	45	65	562(0) 558(7) 560(15)	1.294	1.260	0.034	1.33	0.0985
	3A	45	65	561(0) 555(7) 556(15)	1.853	1.876	0.037	1.62	0.112
5	13	55	55	512(0) 509(7) 510(15)	2.895	2.837	0.058	1.94	0.156
	13A	55	55	513(0) 508(7) 511(15)	2.669	2.604	0.065	2.18	0.168
6	8	55	69	581(0) 564(7) 541(15	2.063	2.001	0.062	1.93	0.162
	8A	55	69	578(0) 569(7) 548(15)	1.881	1.815	0.066	2.23	0.202

.n.	R.No.	Voltage (Volts)	Temperature (°C)	Average Conductivity (mmho/cm) (t)	Initial weight (g) w_1	Final weight (g) w_2	M.R. w_1-w_2 (g)	Machine depth (mm)	Feed(mm/min.)
7	2	65	45	472(0) 470(7) 463(15)	2.609	2.538	0.071	2.43	0.202
	2A	65	45	465(0) 470(7) 471(15)	2.664	2.585	0.079	2.63	0.216
8	4	65	65	565(0) 563(7) 560(15)	1.971	1.884	0.087	2.82	0.213
	4A	65	65	561(0) 562(7) 563(15)	1.810	1.712	0.098	3.15	0.225
9	7	55	41	462(0) 458(7) 456(15)	1.410	1.366	0.044	1.33	0.148
	7A	55	41	459(0) 461(7) 460(15)	2.408	2.359	0.049	1.54	0.162
0	6	69	55	514(0) 509(7) 512(15)	2.320	2.213	0.107	3.15	0.221
	6A	69	55	508(0) 514(7) 513(15)	3.147	3.022	0.135	3.41	0.256
11	9	55	55	514(0) 507(7) 510(15)	2.370	2.319	0.051	1.75	0.154
	9A	55	55	512(0) 509(7) 510(15)	2.210	2.152	0.058	2.04	0.168
12	10	55	55	513(0) 508(7) 511(15)	2.258	2.209	0.049	1.67	0.156
	10A	55	55	509(0) 510(7) 512(15)	2.023	1.964	0.054	2.06	0.169
13	12	55	55	512(0) 508(7) 507(15)	2.167	2.114	0.053	1.72	0.158
	12A	55	55	509(0) 510(7) 512(15)	2.653	2.593	0.060	2.01	0.168

Table D.2 : Experimental values for alumina

p.n.	R.No.	Voltage (Volts)	Temperature (°C)	Average Conductivity (mmho/cm) (t)	Initial weight (g) w_1	Final weight (g) w_2	M.R. w_1-w_2 (g)	Machine depth (mm)	Feed(mm/min.)
1	5	50	55	519(0) 512(15) 513(30)	1.438	1.435	0.003	0.03	0.615
	5A	50	55	520(0) 513(15) 516(30)	1.424	1.419	0.006	0.11	0.0825
2	1	55	45	471(0) 473(15) 469(30)	1.443	1.438	0.005	0.05	0.085
	1A	55	45	475(0) 466(15) 460(30)	1.450	1.441	0.009	0.14	0.09
3	3	60	41	462(0) 458(15) 450(30)	1.429	1.424	0.005	0.04	0.09
	3A	60	41	461(0) 458(15) 453(30)	1.436	1.427	0.009	0.19	0.105
4	7	55	65	561(0) 558(15) 555(30)	1.455	1.449	0.006	0.06	0.09
	7A	55	65	560(0) 555(15) 550(30)	1.438	1.427	0.011	0.16	0.105

p.n.	R.No.	Voltage (Volts)	Temperature (°C)	Average Conductivity (mmho/cm) (t)	Initial weight (g) w_1	Final weight (g) w_2	M.R. w_1-w_2 (g)	Machine depth (mm)	Feed(mm/min.)
5	11	60	55	519(0) 515(15) 510(30)	1.447	1.440	0.007	0.07	0.09
	11A	60	55	521(0) 513(15) 511(30)	1.451	1.437	0.014	0.26	0.11
6	2	65	45	473(0) 470(15) 465(30)	1.437	1.429	0.008	0.16	0.09
	2A	65	45	474(0) 465(15) 460(30)	1.444	1.431	0.013	0.37	0.117
7	4	65	65	560(0) 554(15) 552(30)	1.438	1.426	0.012	0.18	0.096
	4A	65	65	561(0) 555(15) 553(30)	1.428	1.412	0.016	0.44	0.12
8	6	70	55	514(0) 510(15) 513(30)	1.460	1.444	0.016	0.25	0.105
	6A	70	55	514(0) 509(15) 511(30)	1.446	1.426	0.020	0.47	0.123
9	8	60	69	579(0) 562(15) 539(30)	1.430	1.424	0.006	0.06	0.09
	8A	60	69	575(0) 556(15) 534(30)	1.450	1.438	0.012	0.26	0.113
10	9	60	55	511(0) 509(15) 506(30)	1.426	1.418	0.008	0.06	0.09
	9A	60	55	513(0) 511(15) 509(30)	1.458	1.445	0.013	0.25	0.11

Appendix – E

The electrolyte conductivity of NaOH at 18 C with the percentage of concentration by wt of electrolyte is given in the following Figure.